Cellular Electrodynamics

Santiago Ramón y Cajal (1852-1934)

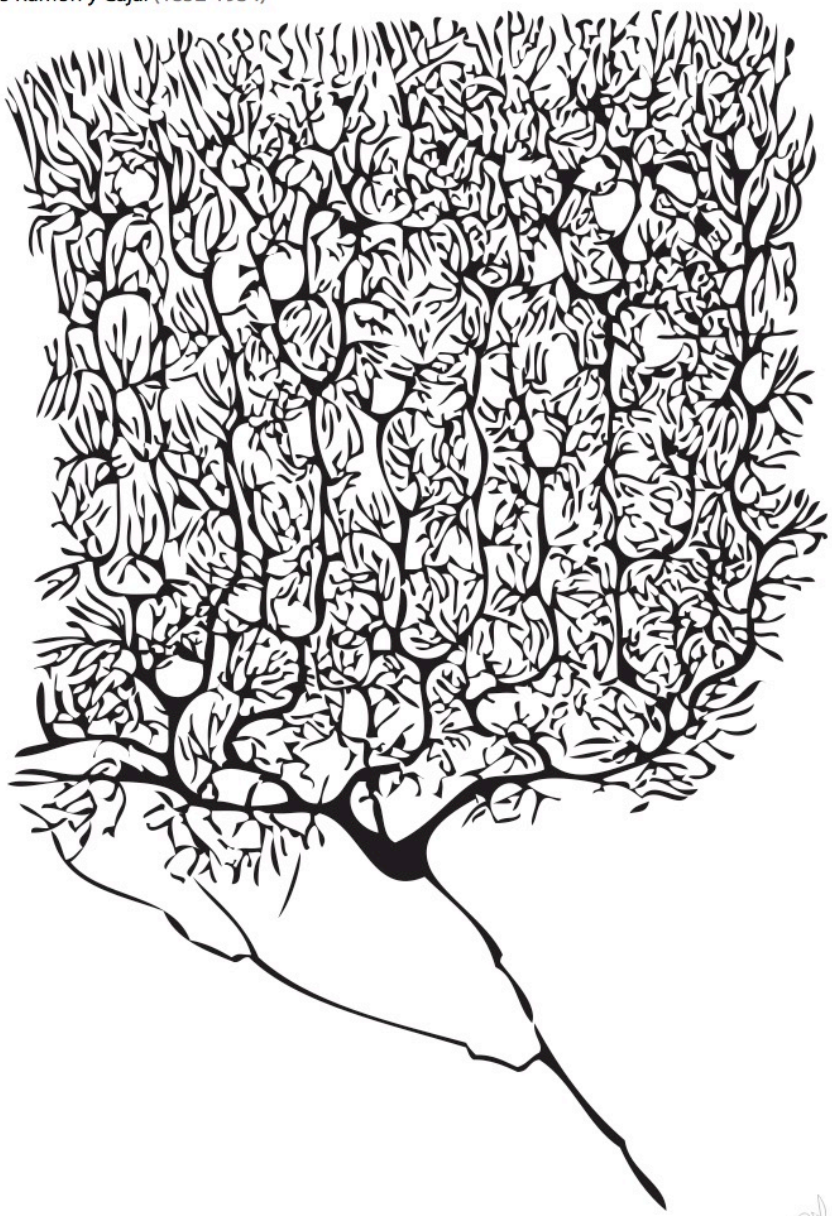

Instructor:
Prof. Christopher Bergevin (cberge@yorku.ca)

Website:
http://www.yorku.ca/cberge/4080W2020.html

York University
Winter 2020
BPHS 4080 Lecture 6

Reference/Acknowledgement:
- TF Weiss (Cellular Biophysics)
- D Freeman

Biophysical Journal *118*, 273–275, January 21, 2020

Biophysical *Journal*

New and Notable

On the Long and Winding Road to a Perfect Membrane Model

Milka Doktorova[1,*]
[1]Department of Integrative Biology and Pharmacology, University of Texas Health Science Center at Houston, Houston, Texas

6. Markones, M., A. Fippel, …, H. Heerklotz. 2020. Stairway to asymmetry: five steps to lipid-asymmetric proteoliposomes. *Biophys. J.* 118:294–302.

Molecular interactions at and within cellular membranes are at the heart of many biological processes. Studying these interactions in their native environment is often challenging because of the inherent complexity of the cellular milieu. Model systems can fill a crucial niche by simplifying the interactome to a few key components, enabling elucidation of the functional contribution of different factors by systematically varying parameters of interest.

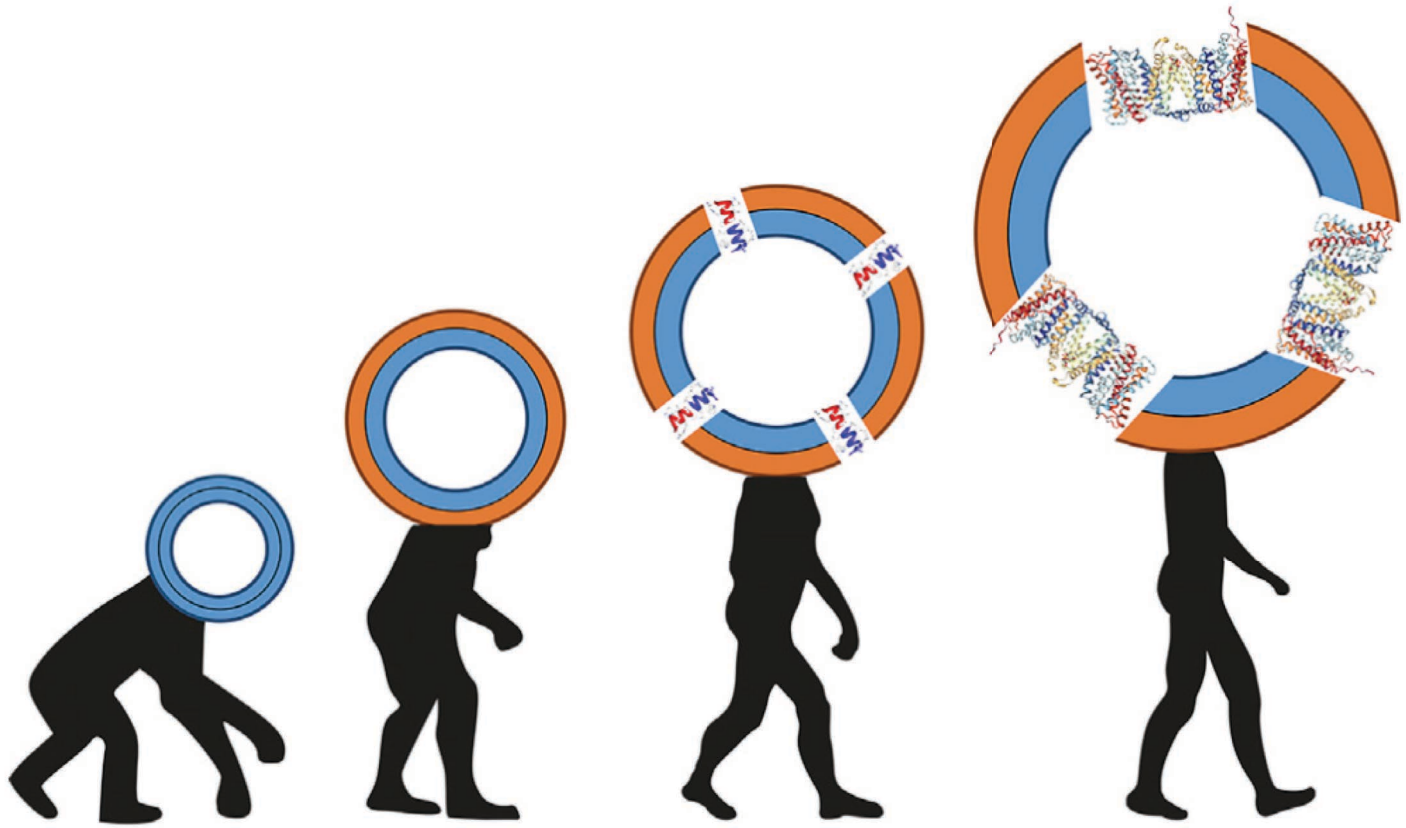

FIGURE 1 Evolution of cell membrane models. To see this figure in color, go online.

Designing an appropriate model requires finding the right balance between simplicity and biological relevance. To study membrane biology, researchers have relied on various approaches to recapitulate key features of cell membranes (Fig. 1). Some used liposomes prepared from total lipid cell extracts to study their interactions with proteins. Liposomes made of synthetic lipids have also been widely used as simpler alternatives to the native membrane protein environment, allowing for better control of membrane components. However, liposomes prepared by traditional methods lack a critical feature of the limiting cellular membrane (i.e., the plasma membrane, or PM), namely the asymmetric distribution of most lipid species between the two membrane leaflets. Life has evolved a sophisticated and carefully orchestrated protein machinery to control this lipid asymmetry and utilize it for various cellular functions. Moreover, this asymmetric transverse organization of lipid components has its own biophysical signature. For example, asymmetry uniquely affects the lipid packing of the two leaflets (1,2), the lateral pressure distribution across the bilayer (3,4), and the membrane electrostatic potential (5). Membrane asymmetry has thus emerged as an important parameter in model studies, especially those focusing on the structure of the PM and its interactions with proteins.

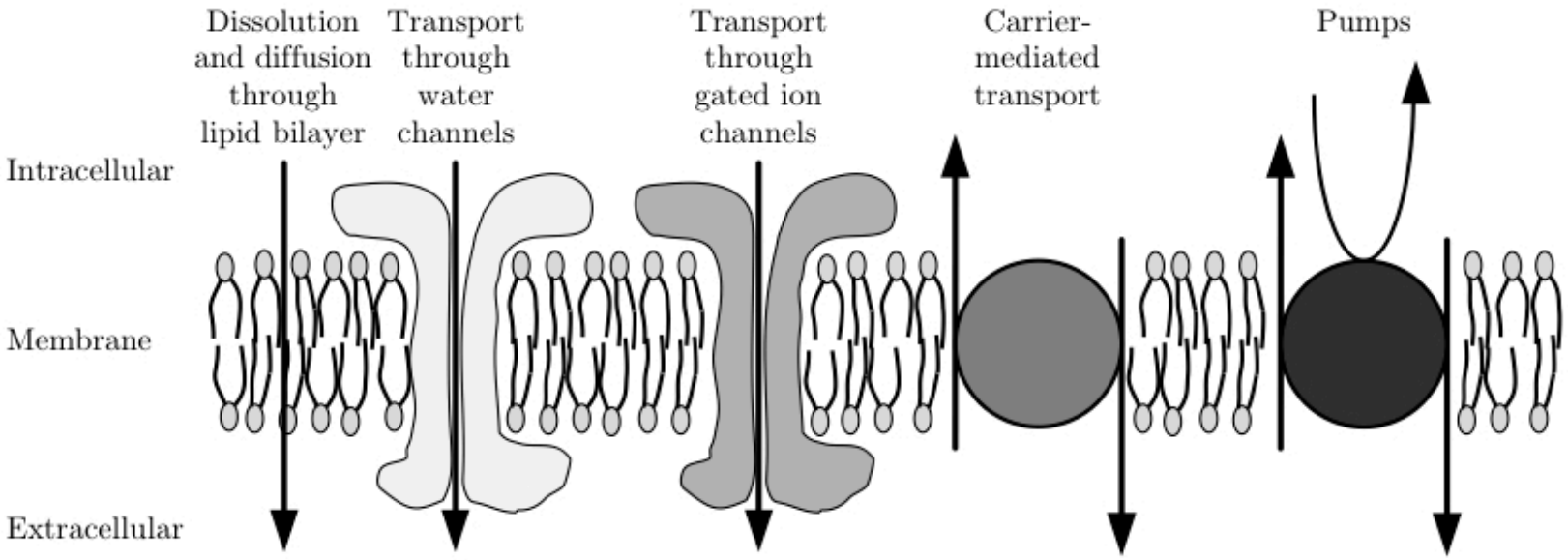
Dissolution and diffusion through lipid bilayer
Transport through water channels
Transport through gated ion channels
Carrier-mediated transport
Pumps
Intracellular
Membrane
Extracellular

Figure 2.19

General Four-State Carrier Model

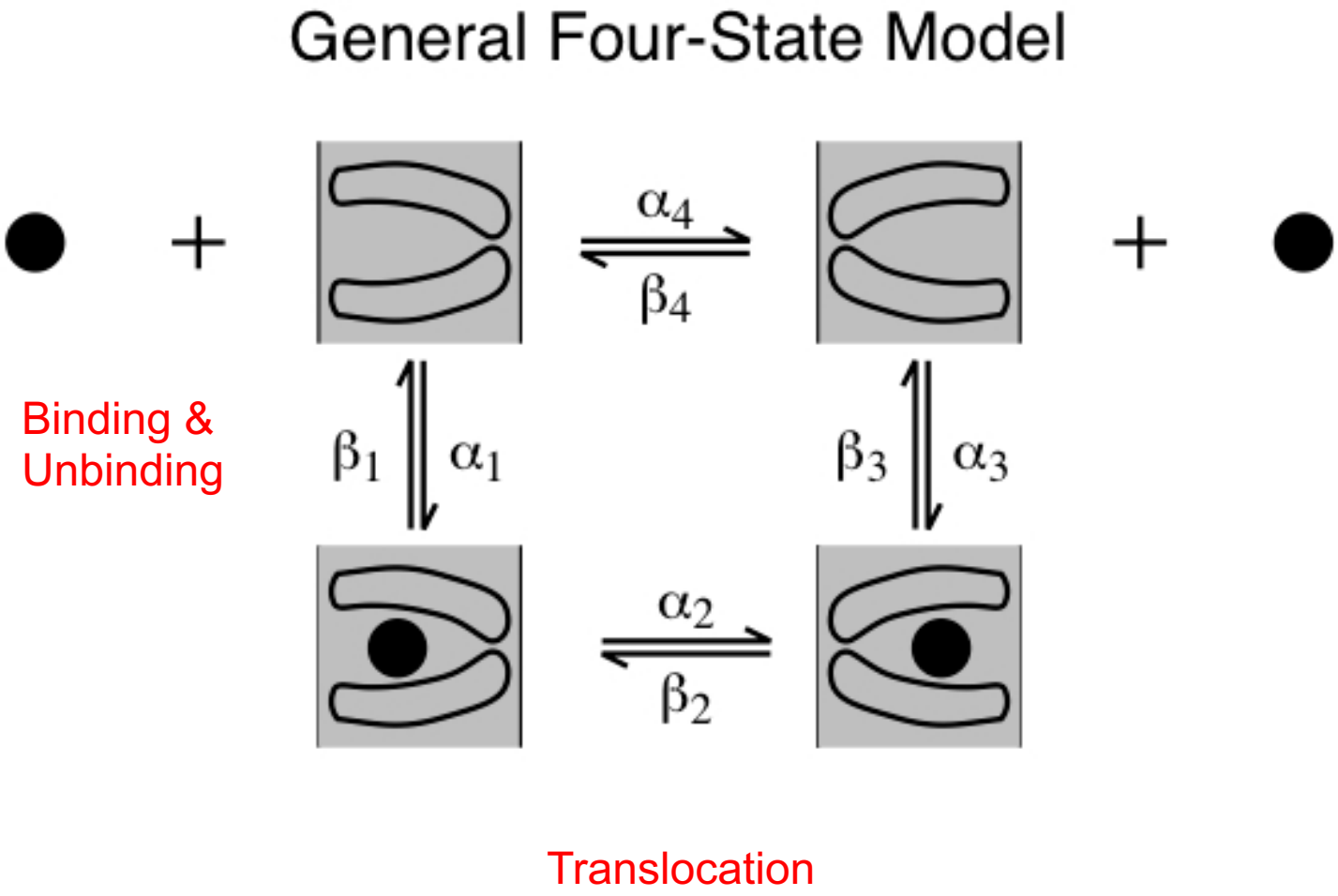

Simple, Symmetric Four-State Model

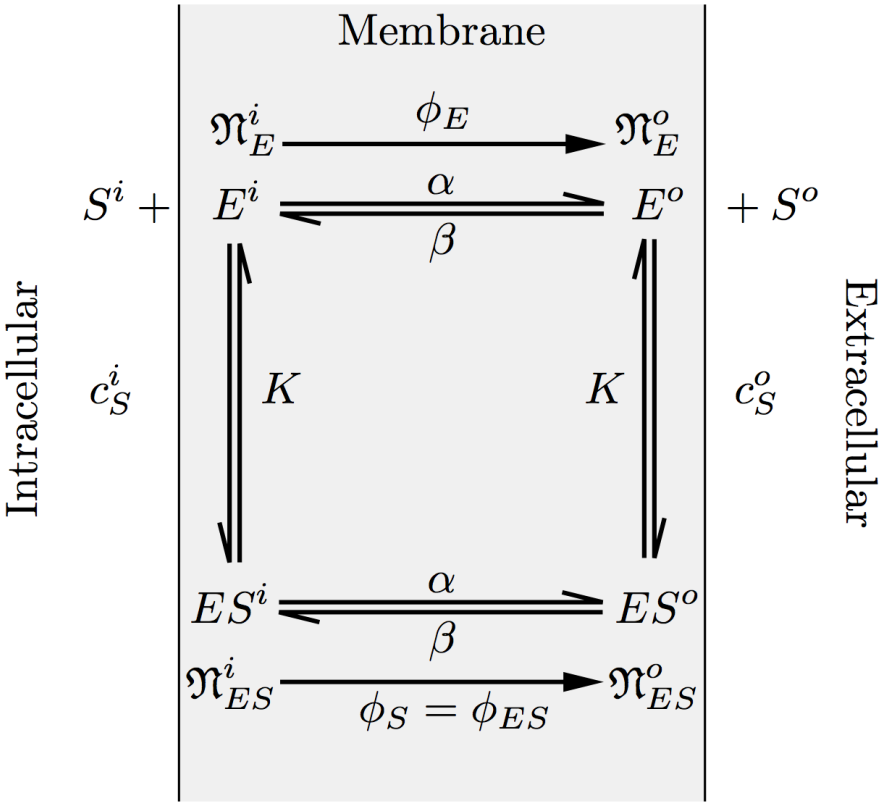

Figure 6.21

1. Conservation of enzyme:

$$\mathfrak{N}_E^i + \mathfrak{N}_E^o + \mathfrak{N}_{ES}^i + \mathfrak{N}_{ES}^o = \mathfrak{N}_{ET}$$

2. Binding is fast (always in steady state):

$$K = \frac{c_S^i \mathfrak{N}_E^i}{\mathfrak{N}_{ES}^i} = \frac{c_S^o \mathfrak{N}_E^o}{\mathfrak{N}_{ES}^o}$$

3. Translocation characterized by fluxes:

$$\phi_{ES} = \alpha \mathfrak{N}_{ES}^i - \beta \mathfrak{N}_{ES}^o$$

$$\phi_E = \alpha \mathfrak{N}_E^i - \beta \mathfrak{N}_E^o$$

4. Net flux of enzyme is zero:

$$\phi_E + \phi_{ES} = 0$$

→ Steady-state

(i.e., carrier densities are independent of time)

Simple, Symmetric Four-State Model

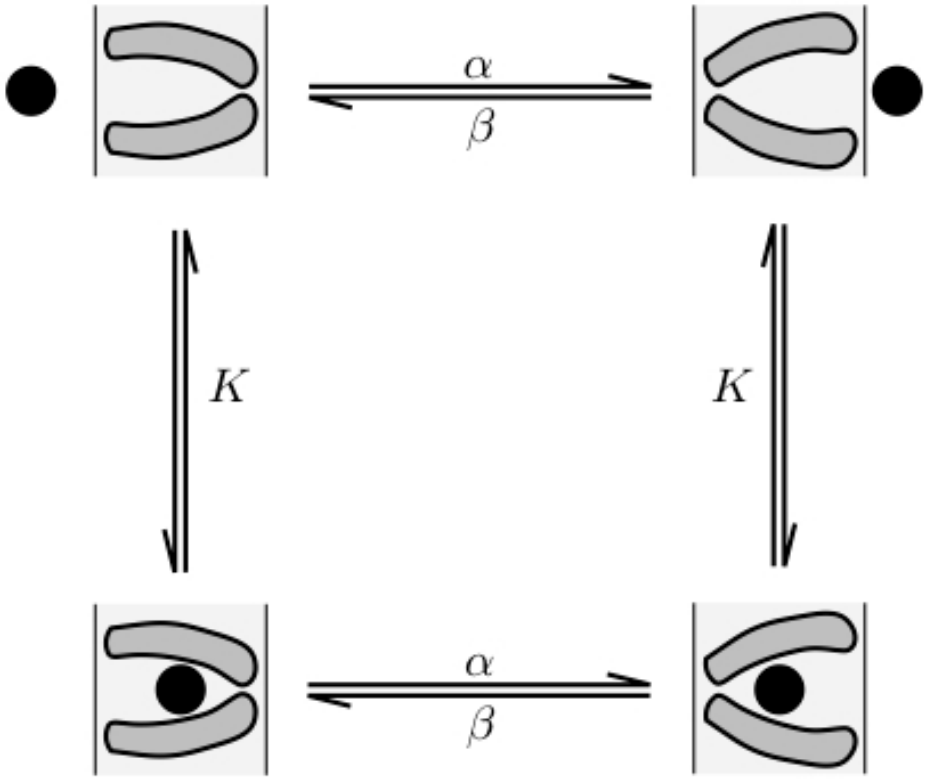

Figure 6.20

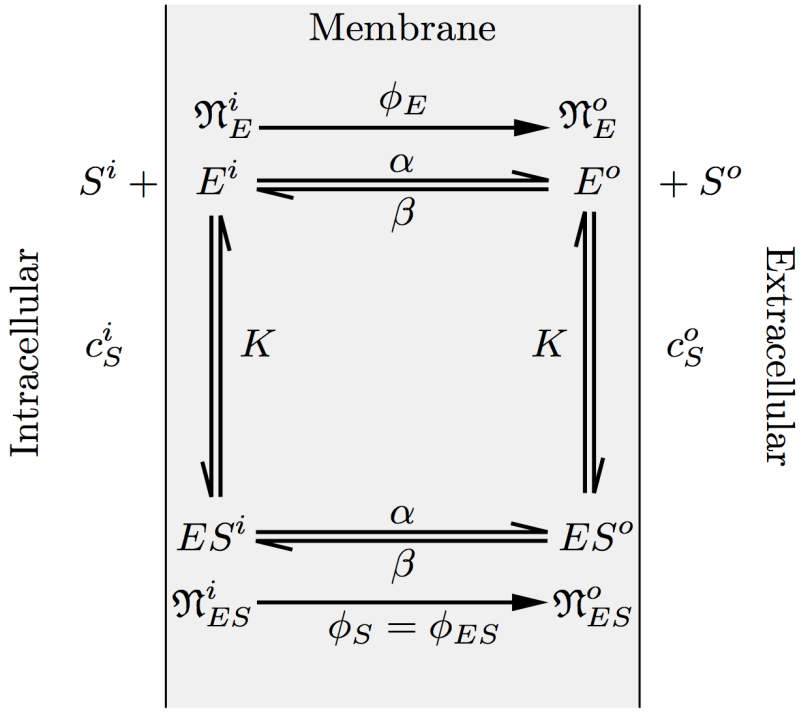

Figure 6.21

Assumption: Steady-state

(i.e., carrier densities are independent of time)

Simple, Symmetric Four-State Model

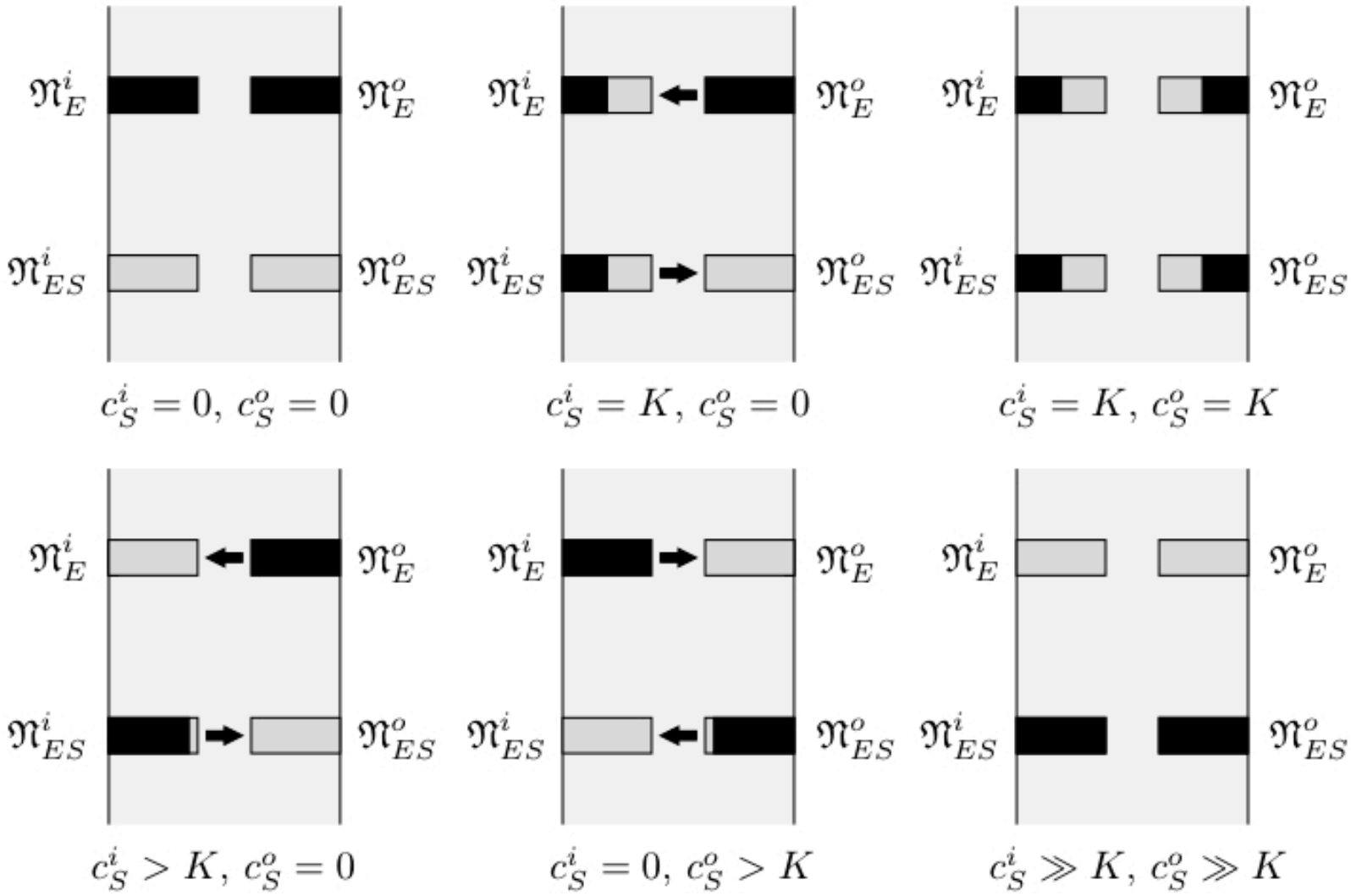

Figure 6.23

Simple, Symmetric Four-State Model

$$\phi_S = (\phi_S)_{max}\left(\frac{c_S^i}{c_S^i + K} - \frac{c_S^o}{c_S^o + K}\right)$$

Total flux

$$(\phi_S)_{max} = \frac{\alpha\beta}{\alpha + \beta}\mathfrak{N}_{ET}$$

$$\overleftarrow{\phi}_S = (\phi_S)_{max}\left(\frac{c_S^o}{c_S^o + K}\right)$$

Influx

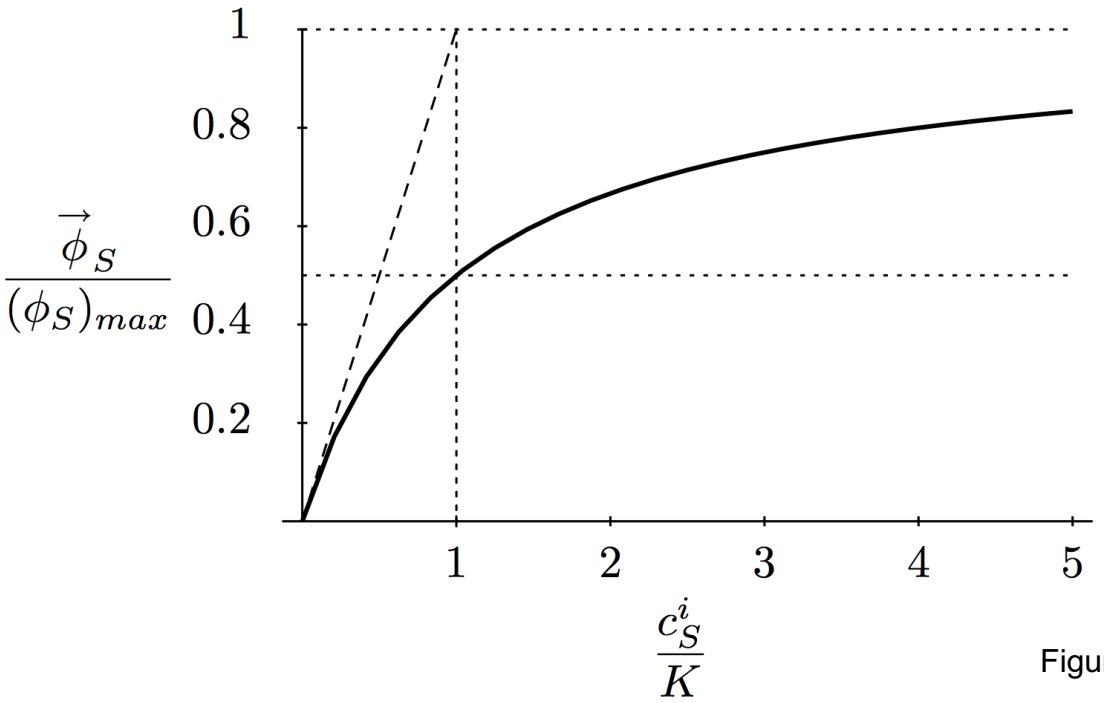

Figure 6.25

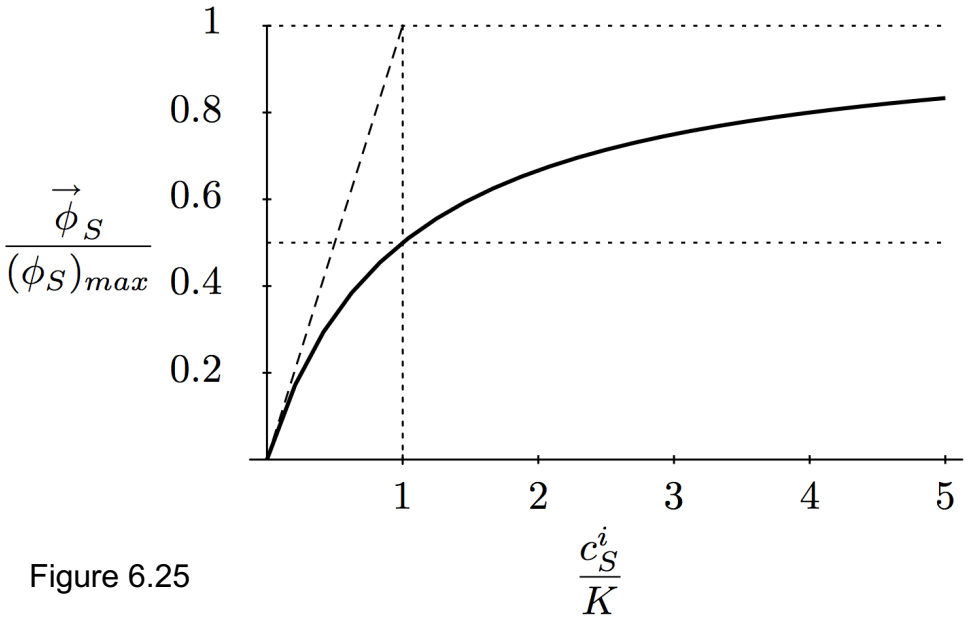

Figure 6.25

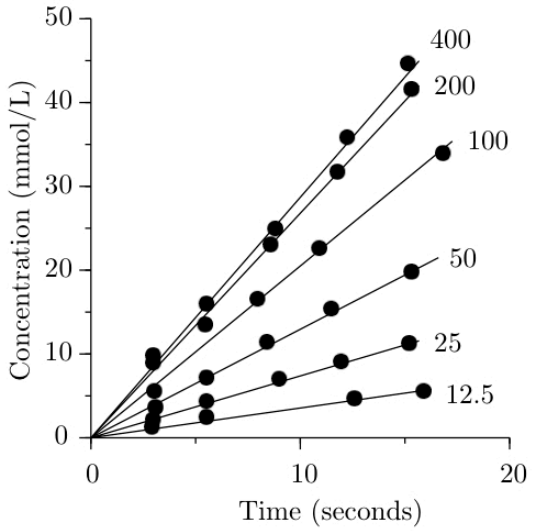

Figure 6.1

→ Carrier model qualitatively explains the data that D&D could not!

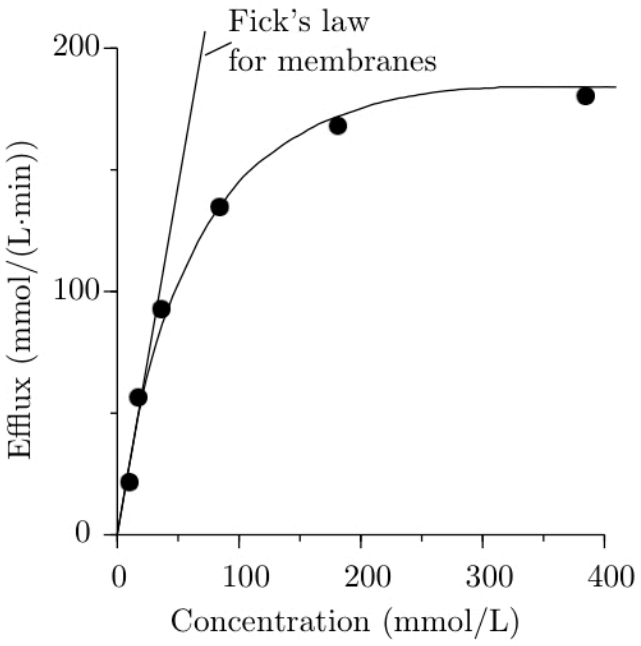

Figure 6.2

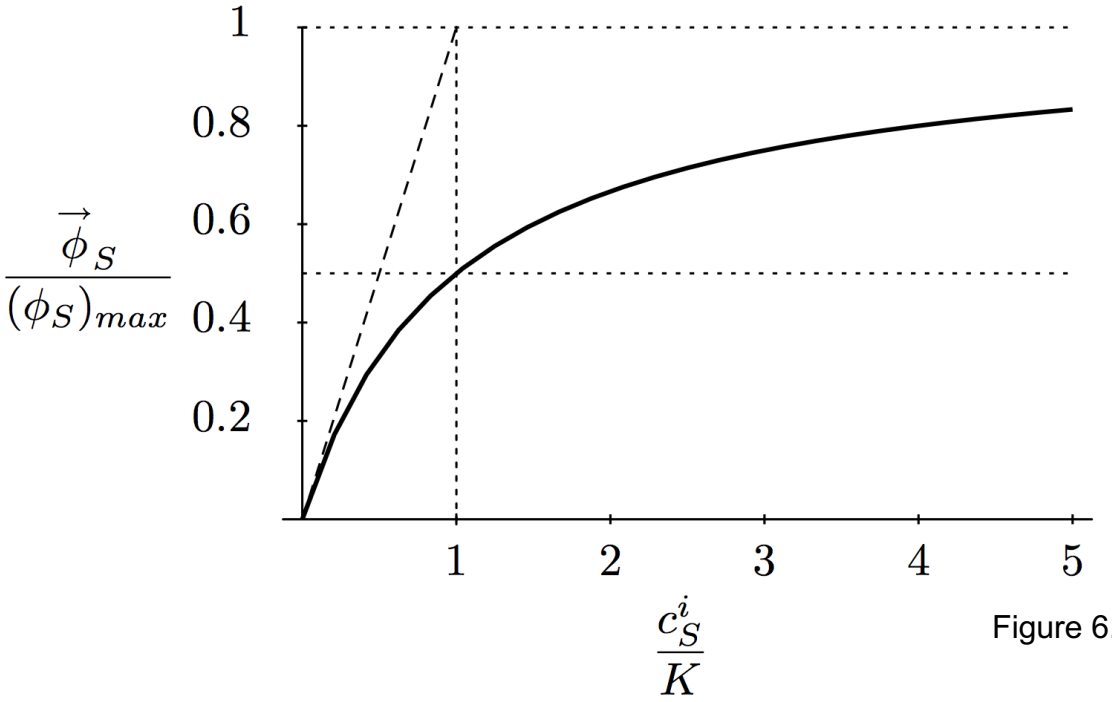

Figure 6.25

→ Linear way to plot nonlinear relationship
(e.g., Lineweaver-Burk plot)

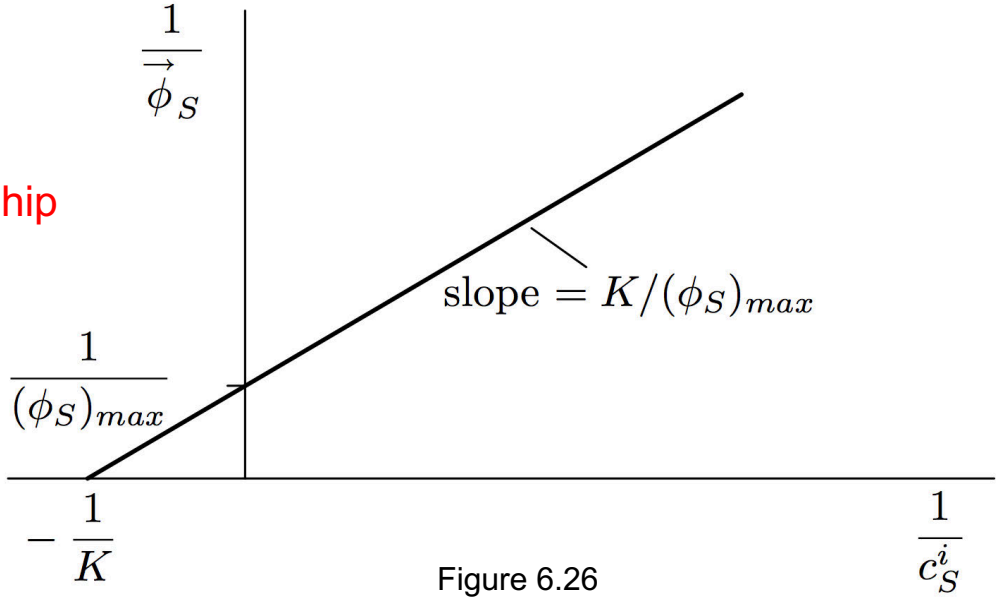

Figure 6.26

Passive Transport: More than diffusion? → Carrier-Mediated Transport

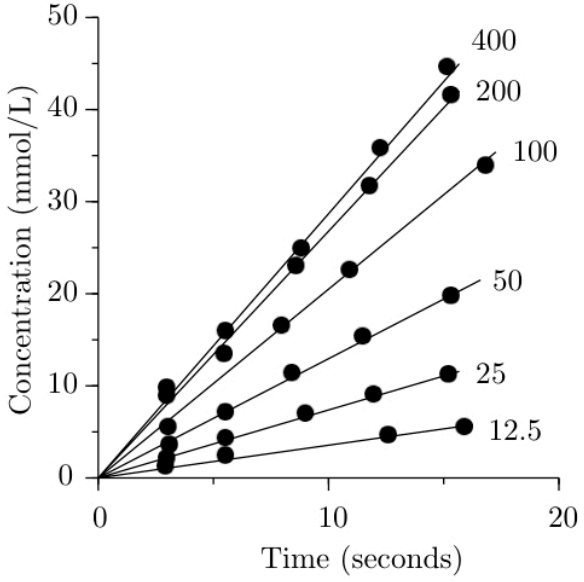

Figure 6.1

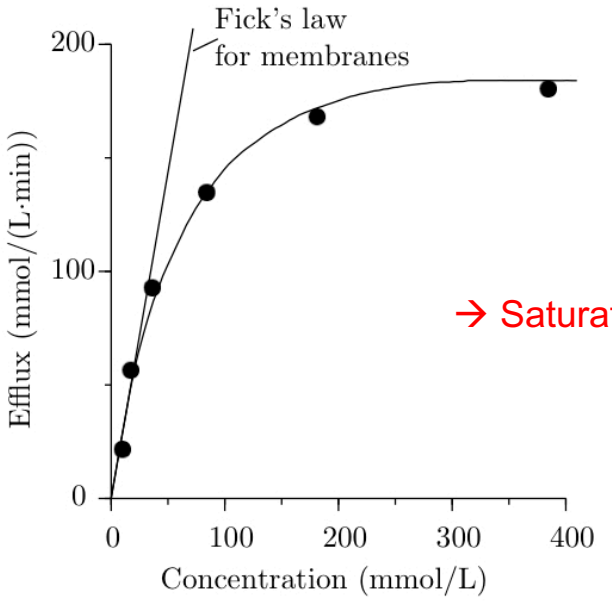

→ Saturation

Figure 6.2

Simple Symetric 4-State Carrier Model

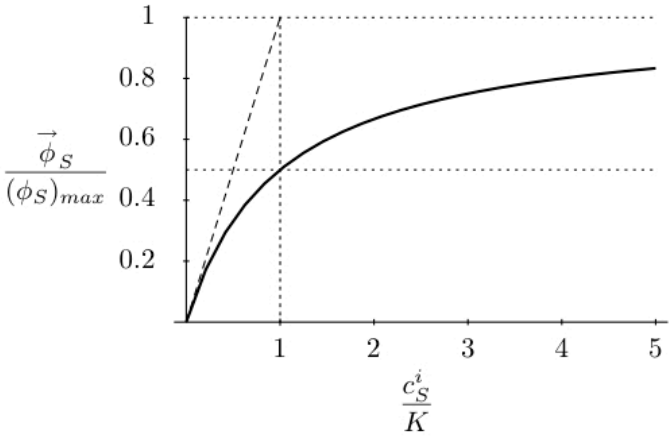

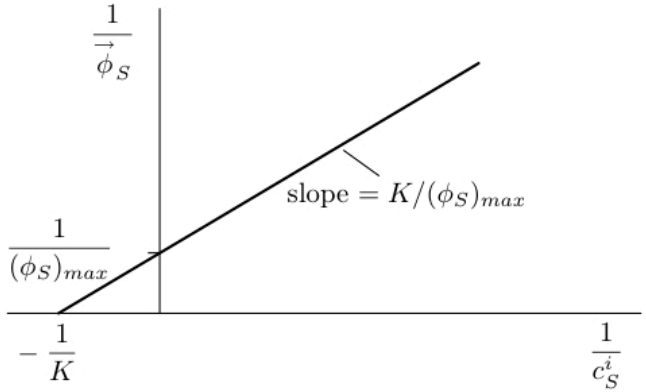

Carrier-Mediated Transport: glucose transporter as example

Distinguishing characteristics of glucose transport:

- facilitated -- i.e., faster than dissolve and diffuse
- structure specific -- different rates for even closely related sugars
- passive -- given a single solute, flow is down concentration gradient
- transport saturates -- solute-solute interactions
- transport can be inhibited -- solute-other interactions
- pharmacology (cytochalasin B)
- hormonal control (insulin)

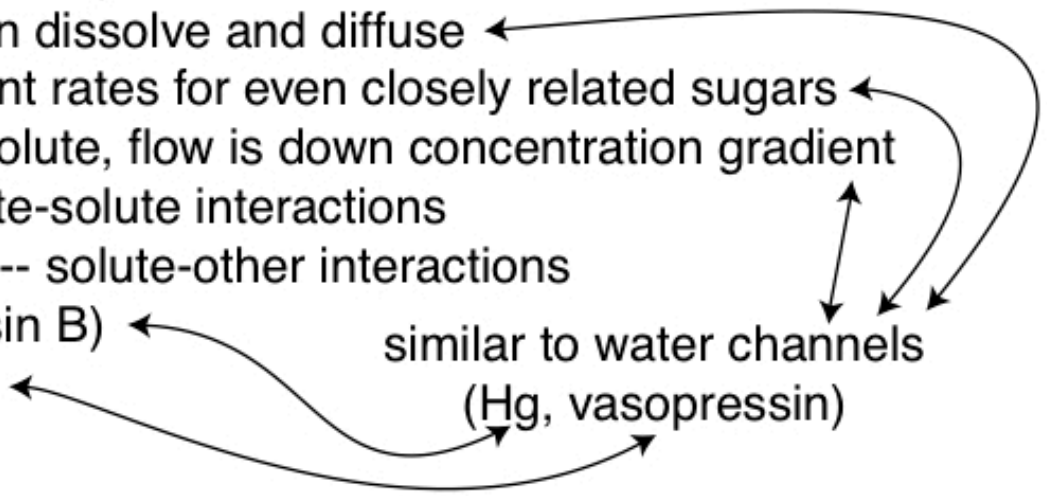

Glucose transport → Important to understand re insulin (e.g., diabetes)

Insulin backbone

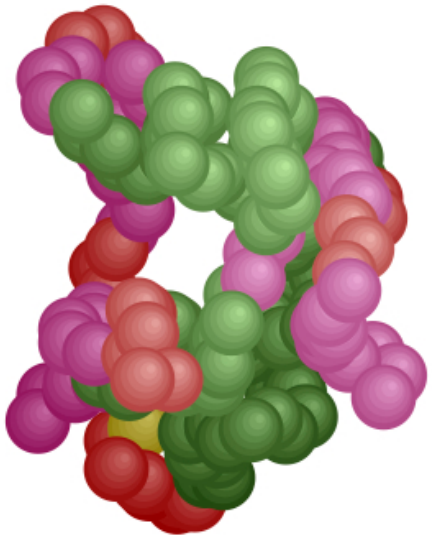

Figure 1.19

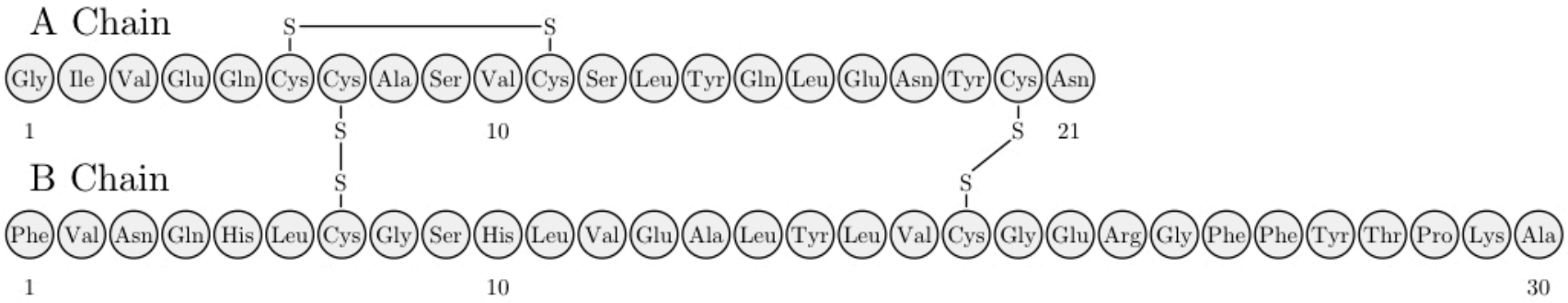

Figure 1.18

Distinguishing characteristics of glucose transport
– are they also characteristic of the simple symmetric 4-state model?

- facilitated: √ solute doesn't need to dissolve in membrane
- structure specific: √ parameters are structure specific
- passive: √ given a single solute, flow is down concentration gradient
- transport saturates: √ rectangular hyperbola
- transport can be inhibited: × need more states
- pharmacology (cytochalasin B): √ similar to inhibition
- hormonal control?

(Selective) Inhibition

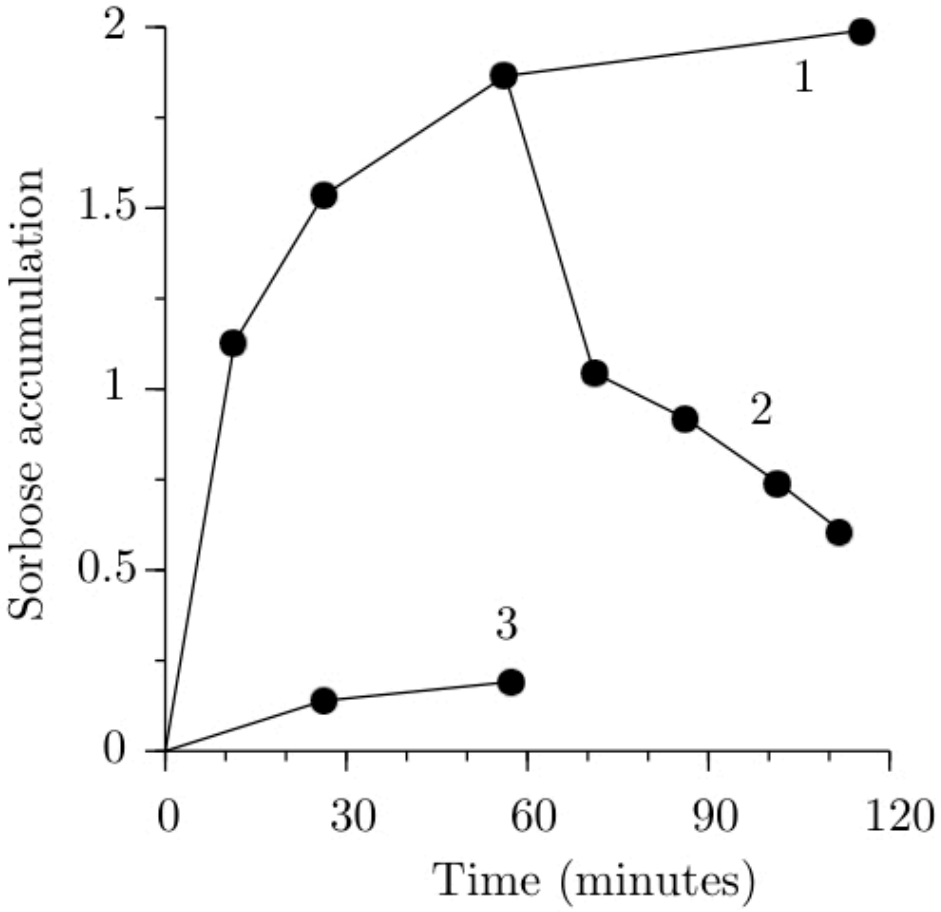

Figure 6.3

→ Glucose inhibits sorbose transport

Two solutes

(competition, both transported)

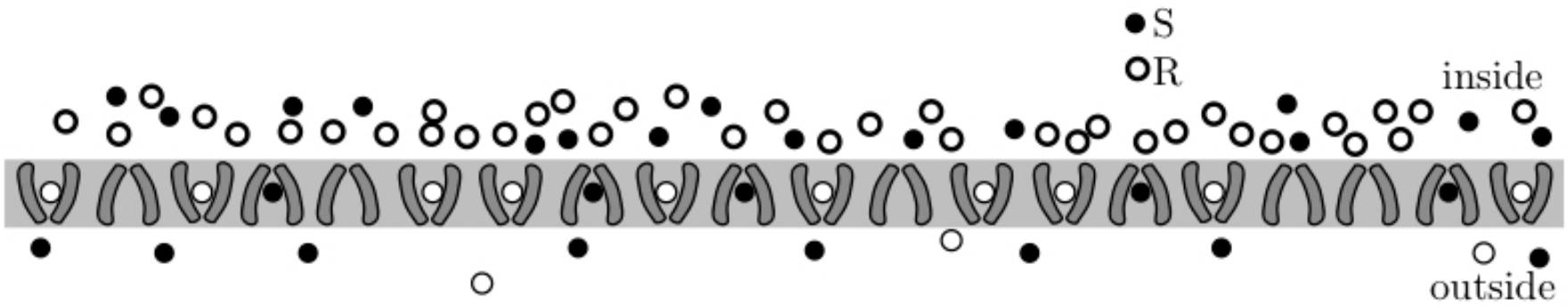

Figure 6.31

Two solutes

(competition, both transported)

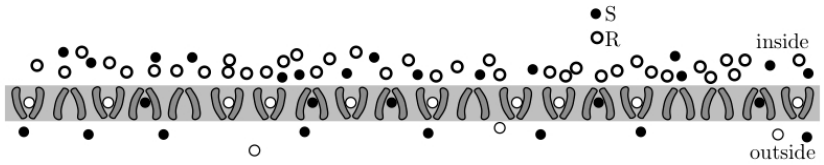

Figure 6.31

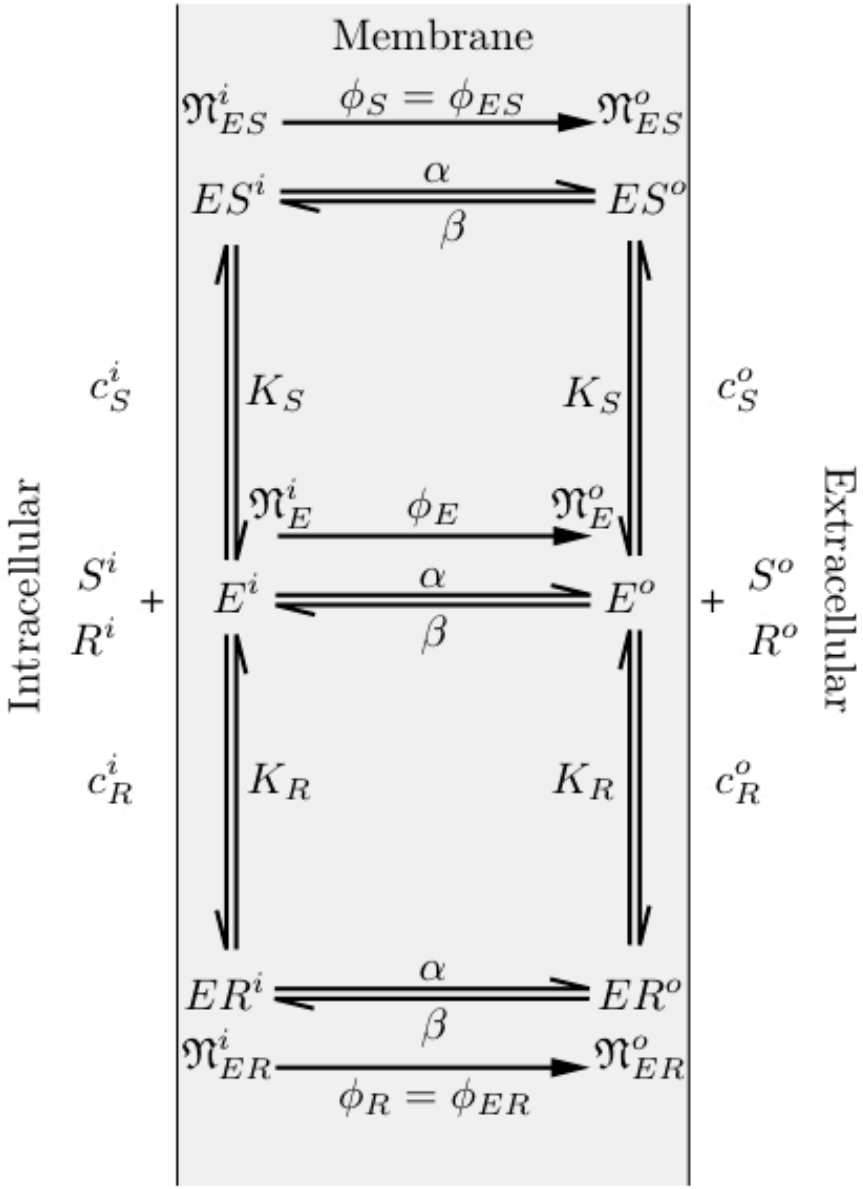

2 Solutes

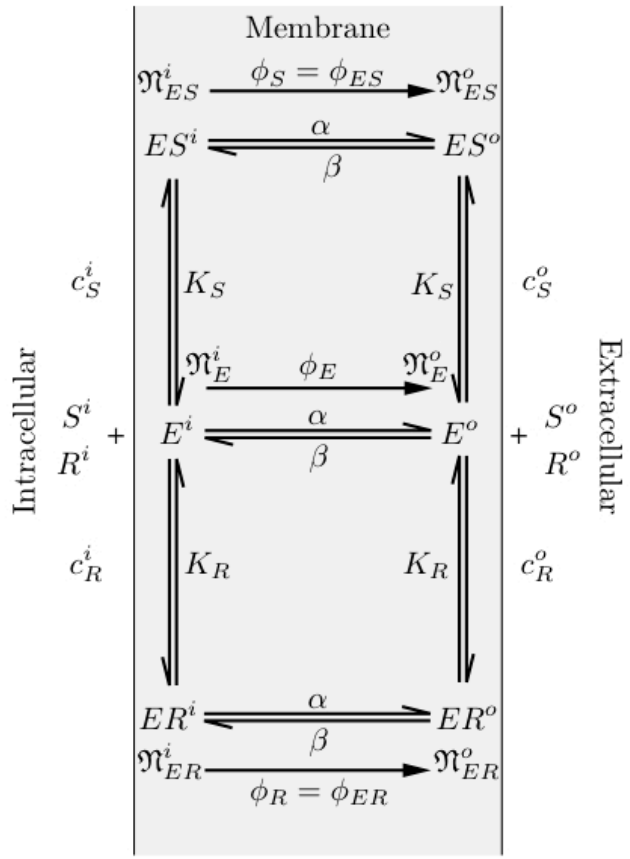

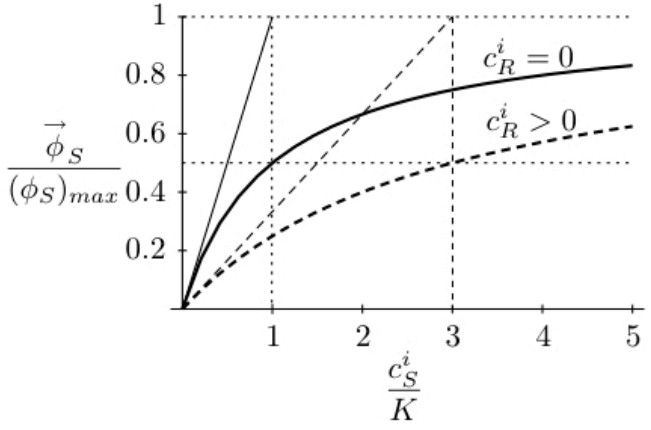

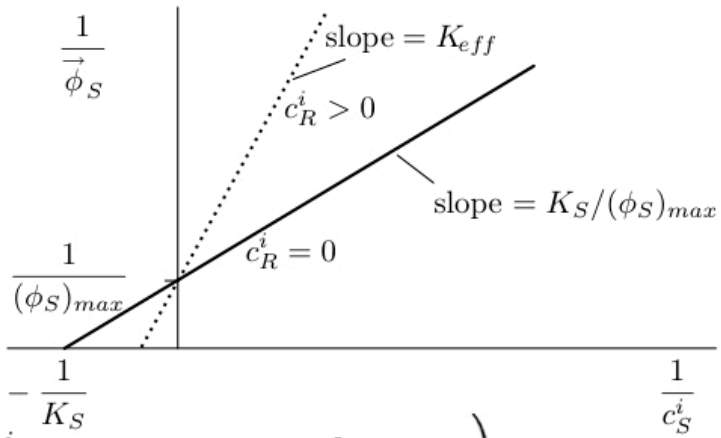

$$\phi_S = (\phi_S)_{max}\left(\frac{c^i_S}{c^i_S + K_S(1+\frac{c^i_R}{K_R})} - \frac{c^o_S}{c^o_S + K_S(1+\frac{c^o_R}{K_R})}\right)$$

$$\overleftarrow{\phi}_S = (\phi_S)_{max}\left(\frac{c^o_S}{c^o_S + K_S\left(1+\frac{c^o_R}{K_R}\right)}\right) = (\phi_S)_{max}\left(\frac{c^o_S}{c^o_S + K_{eff}}\right)$$

$$K_{eff} = K_S\left(1+\frac{c^o_R}{K_R}\right)$$

1 Solute + 1 Competitive Inhibitor

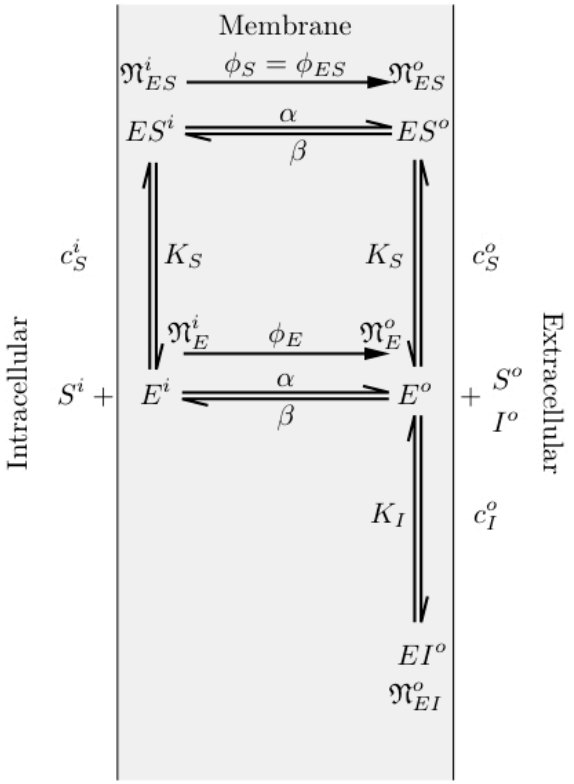

$$\overleftarrow{\phi}_S = (\phi_S)_{max}\left(\frac{c^o_S}{c^o_S + K_S\left(1+\frac{\alpha}{\alpha+\beta}\frac{c^o_I}{K_I}\right)}\right)$$

$$\overleftarrow{\phi}_S = (\phi_S)_{max}\left(\frac{c^o_S}{c^o_S + K_{eff}}\right)$$

$$K_{eff} = K_S\left(1+\frac{\alpha}{\alpha+\beta}\frac{c^o_I}{K_I}\right)$$

1 Solute + 1 Noncompetitive Inhibitor

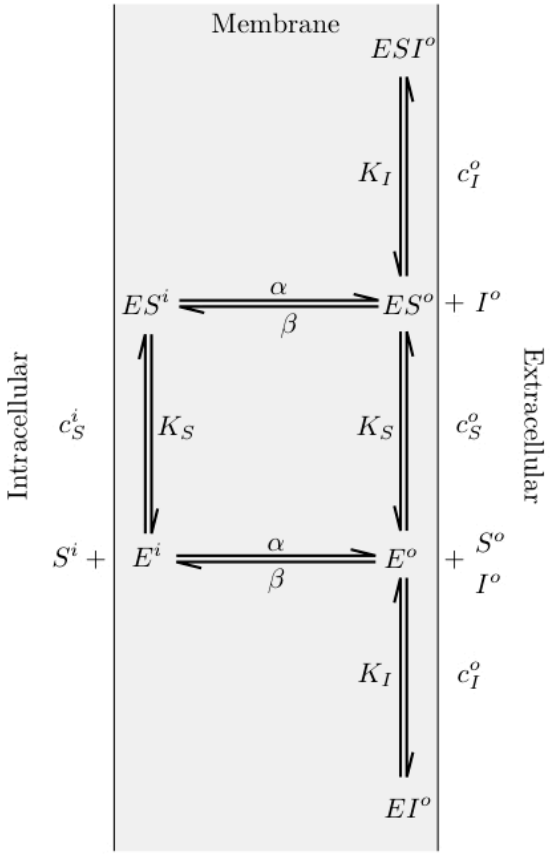

$$\overleftarrow{\phi}_S = \mathfrak{N}_{ET}\left(\frac{\alpha\beta}{\alpha(\frac{c^o_I}{K_I}+1)+\beta}\right)\left(\frac{c^o_S}{c^o_S + K_S}\right)$$

$$\overleftarrow{\phi}_S = (\phi_S)^{eff}_{max}\left(\frac{c^o_S}{c^o_S + K_S}\right)$$

$$(\phi_S)^{eff}_{max} = \mathfrak{N}_{ET}\left(\frac{\alpha\beta}{\alpha(\frac{c^o_I}{K_I}+1)+\beta}\right)$$

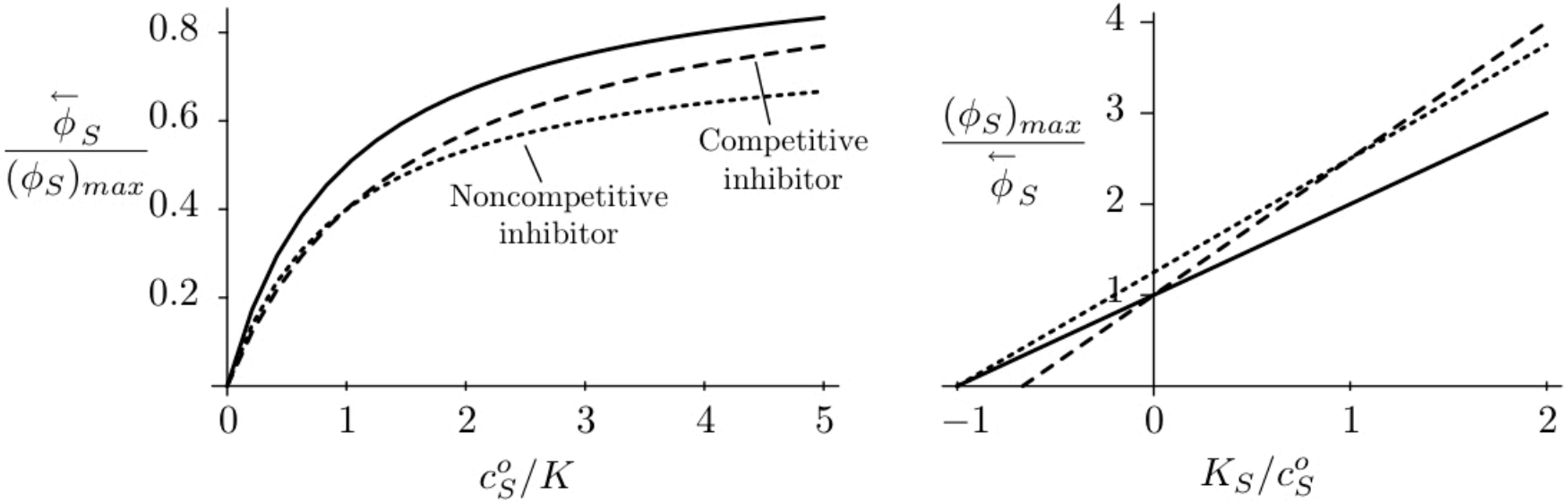

→ Model can be adapted to describe a wide array of behaviors

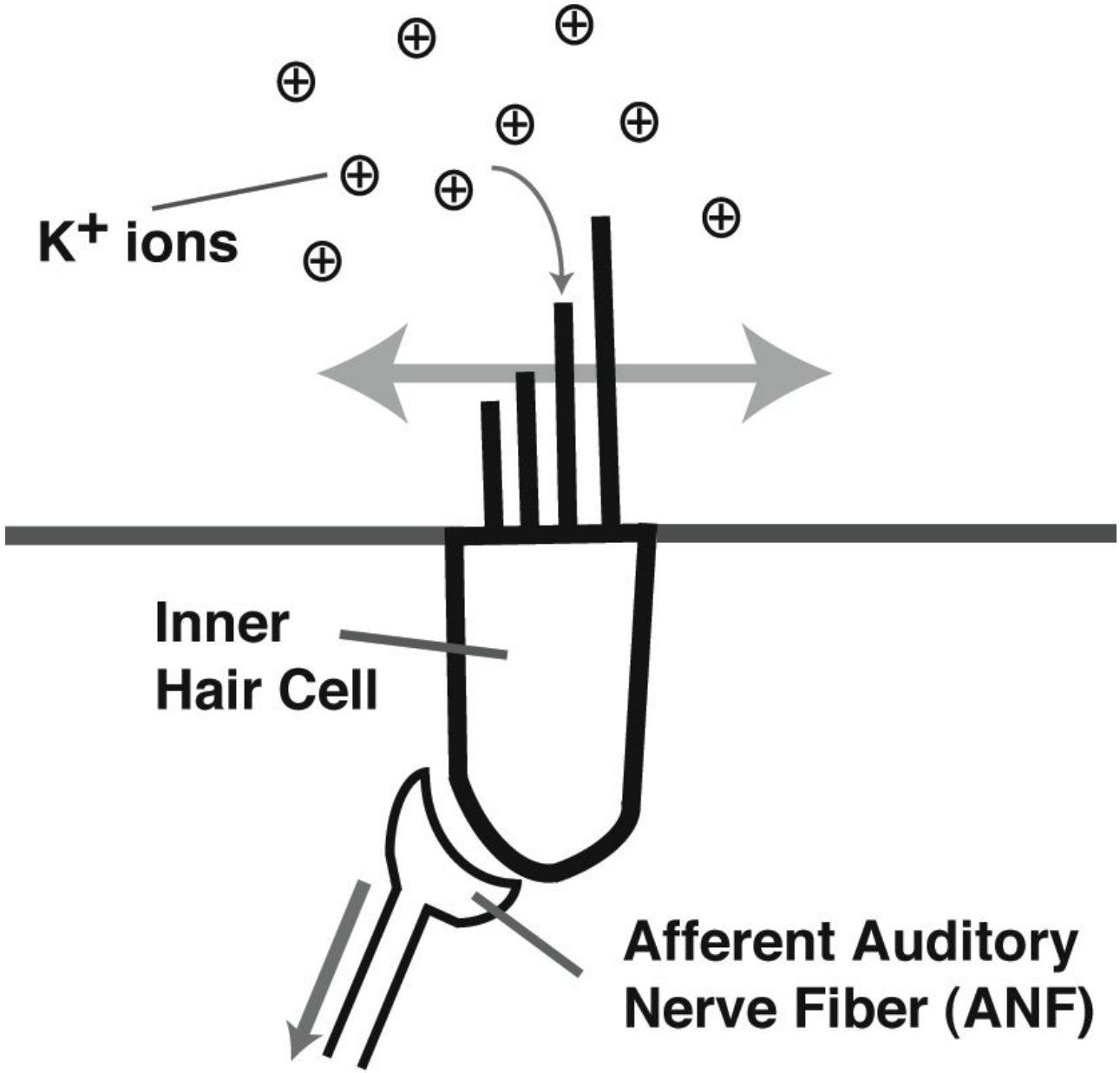
K+ ions
Inner
Hair Cell
Afferent Auditory
Nerve Fiber (ANF)

Proc. Natl. Acad. Sci. USA
Vol. 95, pp. 15321–15326, December 1998
Biophysics

A model for amplification of hair-bundle motion by cyclical binding of Ca^{2+} to mechanoelectrical-transduction channels

YONG CHOE*, MARCELO O. MAGNASCO†, AND A. J. HUDSPETH*‡§

Laboratories of *Sensory Neuroscience and †Mathematical Physics and ‡Howard Hughes Medical Institute, The Rockefeller University, 1230 York Avenue, New York, NY 10021-6399

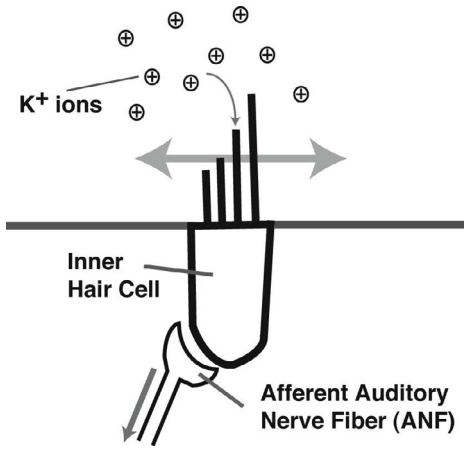

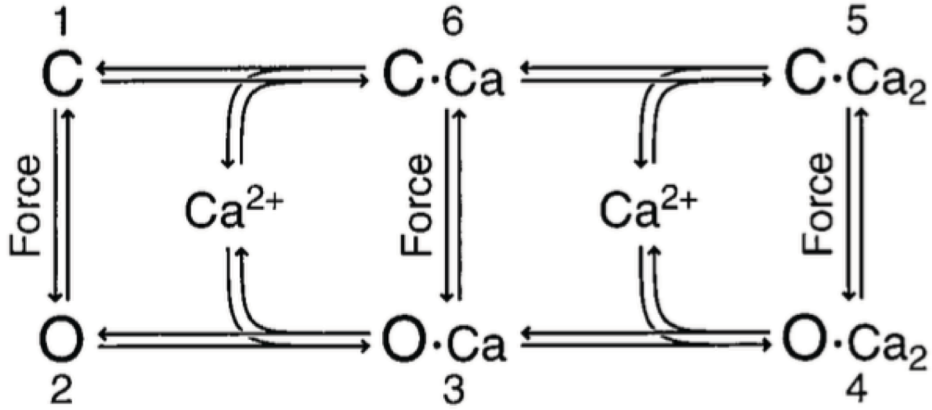

ABSTRACT **Amplification of auditory stimuli by hair cells augments the sensitivity of the vertebrate inner ear. Cell-body contractions of outer hair cells are thought to mediate amplification in the mammalian cochlea. In vertebrates that lack these cells, and perhaps in mammals as well, active movements of hair bundles may underlie amplification. We have evaluated a mathematical model in which amplification stems from the activity of mechanoelectrical-transduction channels. The intracellular binding of Ca^{2+} to channels is posited to promote their closure, which increases the tension in gating springs and exerts a negative force on the hair bundle. By enhancing bundle motion, this force partially compensates for viscous damping by cochlear fluids. Linear stability analysis of a six-state kinetic model reveals Hopf bifurcations for parameter values in the physiological range. These bifurcations signal conditions under which the system's behavior changes from a damped oscillatory response to spontaneous limit-cycle oscillation. By varying the number of stereocilia in a bundle and the rate constant for Ca^{2+} binding, we calculate bifurcation frequencies spanning the observed range of auditory sensitivity for a representative receptor organ, the chicken's cochlea. Simulations using prebifurcation parameter values demonstrate frequency-selective amplification with a striking compressive nonlinearity. Because transduction channels occur universally in hair cells, this active-channel model describes a mechanism of auditory amplification potentially applicable across species and hair-cell types.**

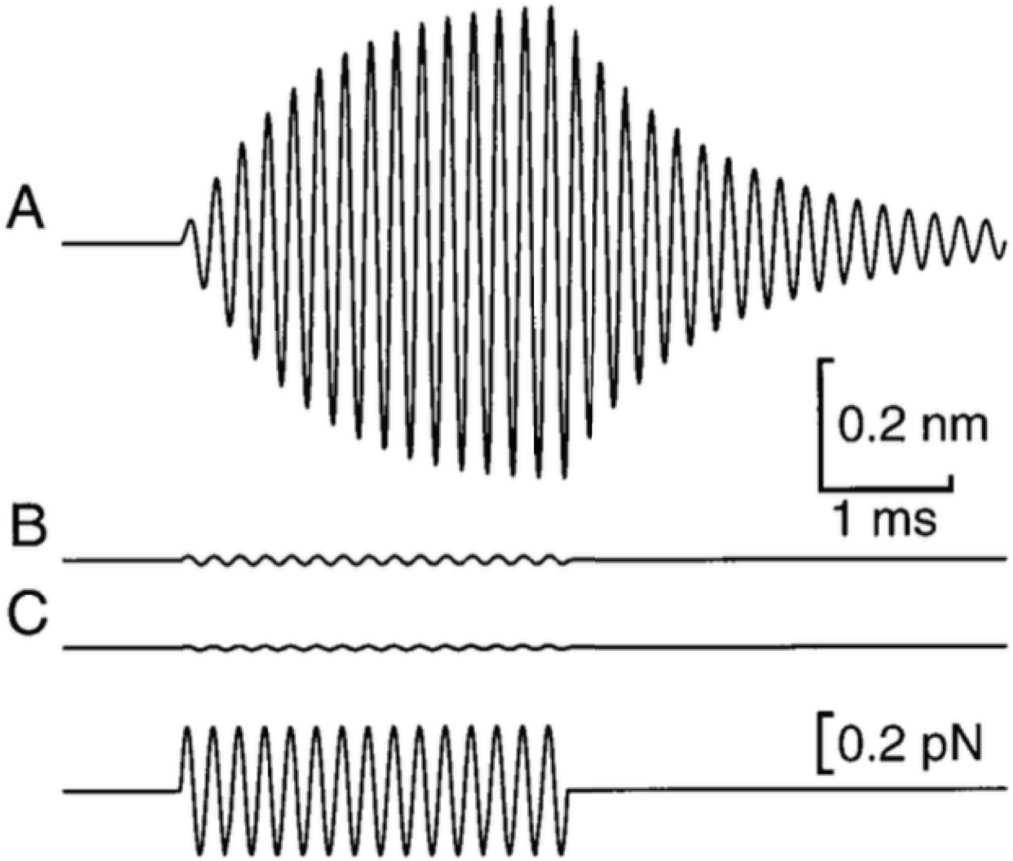

FIG. 1. Schematic diagram of the active-channel model. Each transduction channel is posited to exist in either a closed form, C, or an open one, O. Application of a positive stimulus force to the hair bundle promotes channel opening, whereas binding of Ca^{2+} favors closure. The rate constants for reactions in the counterclockwise direction are designated k_F, those pertaining to the clockwise direction k_R, and those for the two central transitions k_{36}. During sinusoidal stimulation or limit-cycle oscillation, the occupancy of the channel's six states cycles in the counterclockwise direction.

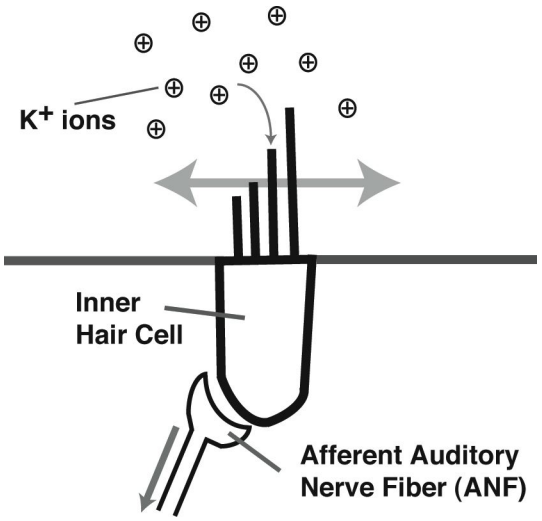

Proc. Natl. Acad. Sci. USA
Vol. 95, pp. 15321–15326, December 1998
Biophysics

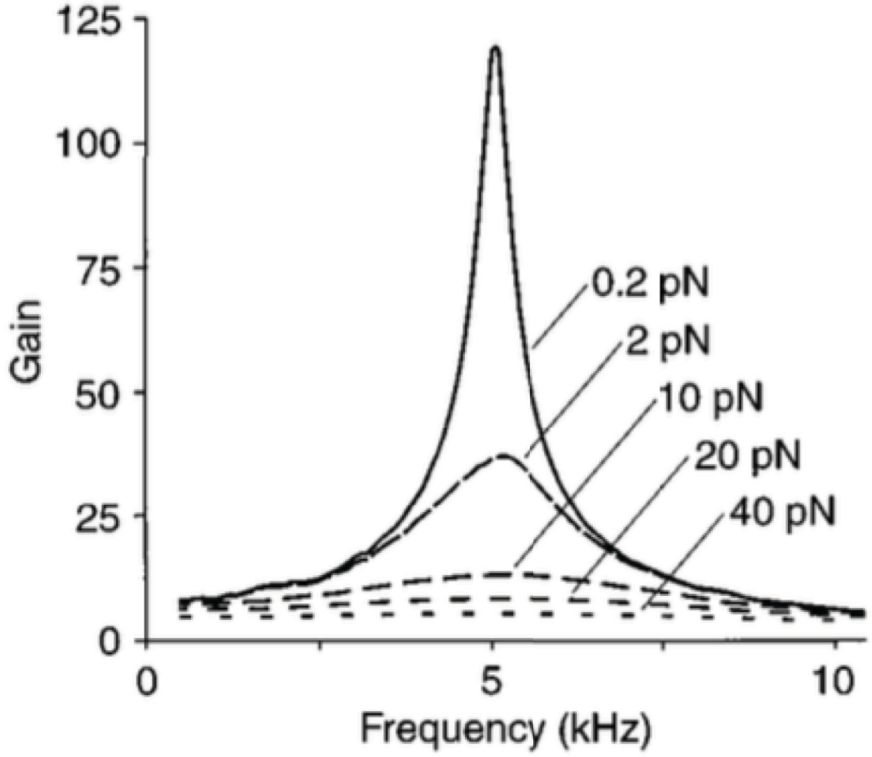

FIG. 4. Modeled responses of a hair bundle to stimulation with a 5-kHz sinusoidal force 0.2 pN in amplitude (*Bottom* trace). (*A*) In the active-channel model, the bundle displays oscillations of roughly threshold amplitude upon stimulation. The system's high Q is revealed by the gradual rise and decline of the response. (*B*) The response of a similar model without Ca^{2+}-induced channel reclosure shows far less amplification and no resonance after stimulation. (*C*) For a passive model without channel gating, the displacement is roughly the driving force divided by the bundle's stiffness. In each instance, $M_{HB} = 60$ pg, $\xi_{HB} = 100$ nN·s·m^{-1}, $K_{SP} = 9{,}000$ μN·m^{-1}, $\kappa_{GS} = 1{,}200$ μN·m^{-1}, $N_S = 210$, $N_T = 184$, $\gamma = 0.50$, $b = 4.5$ nm, $\delta_{12} = 0.9$, $\delta_{36} = 0.1$, $\delta_{45} = 0.1$, $k_F = 93{,}500\ s^{-1}$, $k_R = 10{,}300\ s^{-1}$, and $k_{36} = 0.88\ s^{-1}$. The response in *B* displays an offset of -2.9 nm; the system's bistability around a resting position at which $p_{O,REST} = 0.5$ emerges from fixed-point analysis.

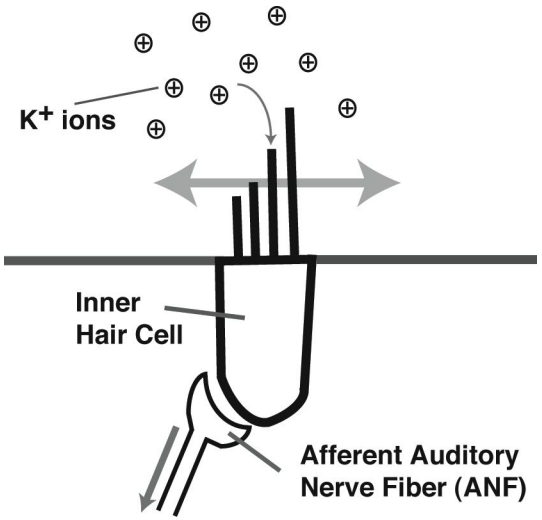

Proc. Natl. Acad. Sci. USA
Vol. 95, pp. 15321–15326, December 1998
Biophysics

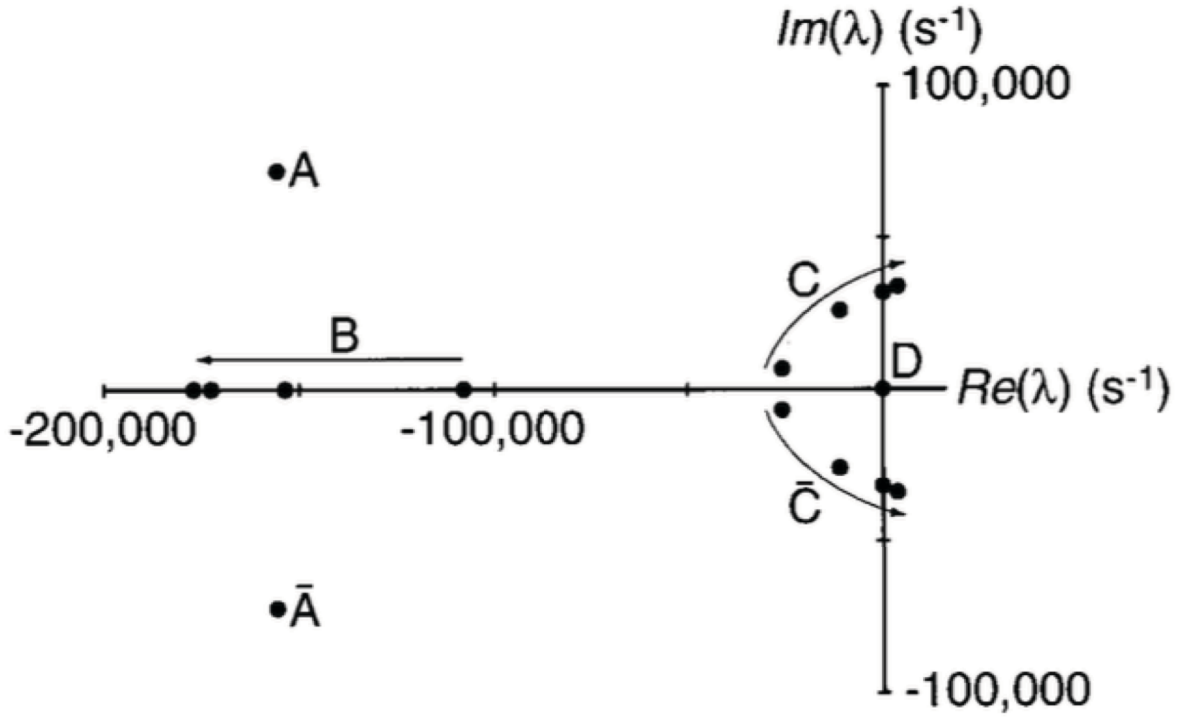

FIG. 2. Parameter dependence of the system's eigenvalues (λ). The eigenvalues determined for four values (108, 140, 220, and 300) of the stereociliary number, N_S, are represented on the complex plane. The points designated B, C, and $\bar{C}$ demonstrate the functional dependence of the system on N_S; the arrows indicate the progression of eigenvalues with increasing values of this parameter. The angular frequency at the Hopf bifurcation for C and $\bar{C}$, $\pm 32{,}000\ s^{-1}$, corresponds to a characteristic frequency of ~5 kHz. Point D, which represents the conservation of state probability in the channel-gating cycle, remains at the origin. The conjugate pair A and $\bar{A}$ are independent of N_S and also appear stationary. An additional conjugate pair of eigenvalues, those farthest to the left, have been omitted to permit display of the remaining points on an informative scale. The system is characterized by an eighth-degree characteristic polynomial that precludes a closed form for the eigenvalues; numerical evaluation was therefore necessary. The stability analysis and simulation programs were written in MATHEMATICA and executed on a Macintosh Quadra 800 computer (Apple Computer, Cupertino, CA) or an Indigo Impact 10000 computer (Silicon Graphics, Mountain View, CA).

Molecular biology to identify glucose transporter

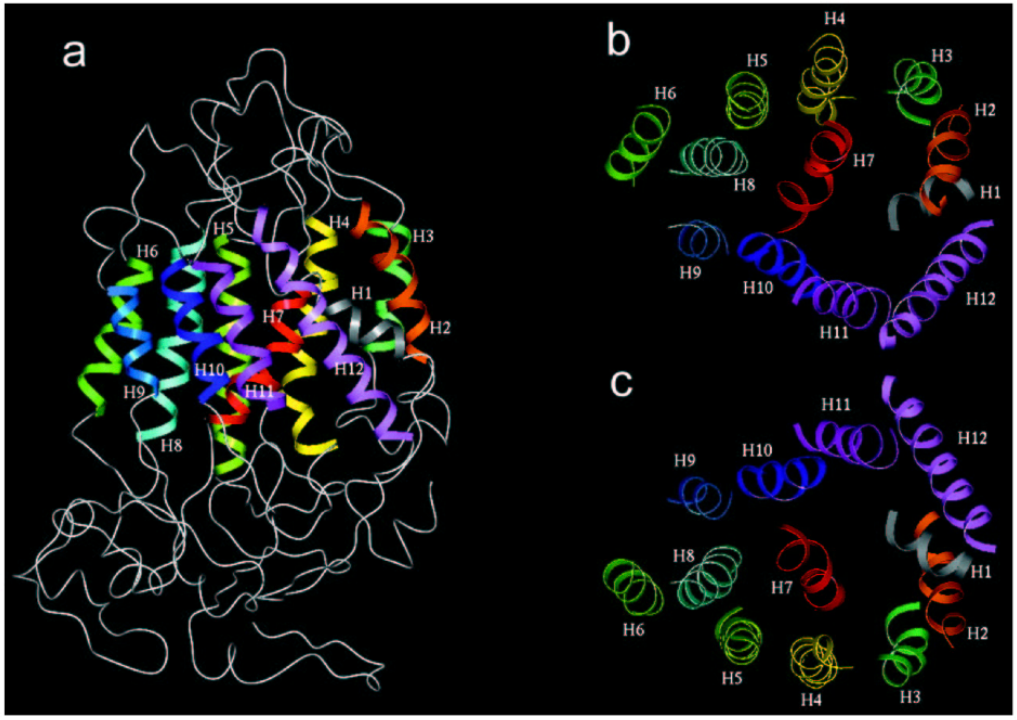

Zuniga, Shi, Haller, Rubashkin, Flynn, Iserovick, and Fischbarg (Nov. 2001)
J. Biological Chemistry 48: 44970-44975.

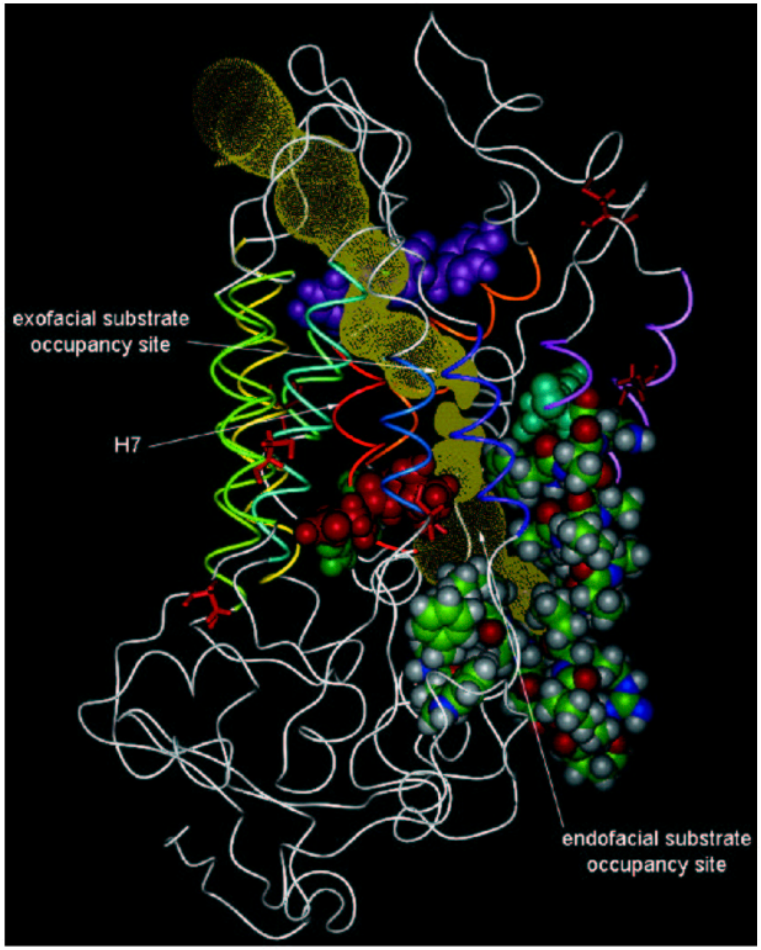

Zuniga, Shi, Haller, Rubashkin, Flynn, Iserovick, and Fischbarg (Nov. 2001)
J. Biological Chemistry 48: 44970-44975.

Cell Metabolism
Review

The GLUT4 Glucose Transporter

Shaohui Huang[1] and Michael P. Czech[1,*]
[1] Program in Molecular Medicine, University of Massachusetts Medical School, Worcester, MA 01605, USA

Few physiological parameters are more tightly and acutely regulated in humans than blood glucose concentration. The major cellular mechanism that diminishes blood glucose when carbohydrates are ingested is insulin-stimulated glucose transport into skeletal muscle. Skeletal muscle both stores glucose as glycogen and oxidizes it to produce energy following the transport step. The principal glucose transporter protein that mediates this uptake is GLUT4, which plays a key role in regulating whole body glucose homeostasis. This review focuses on recent advances on the biology of GLUT4.

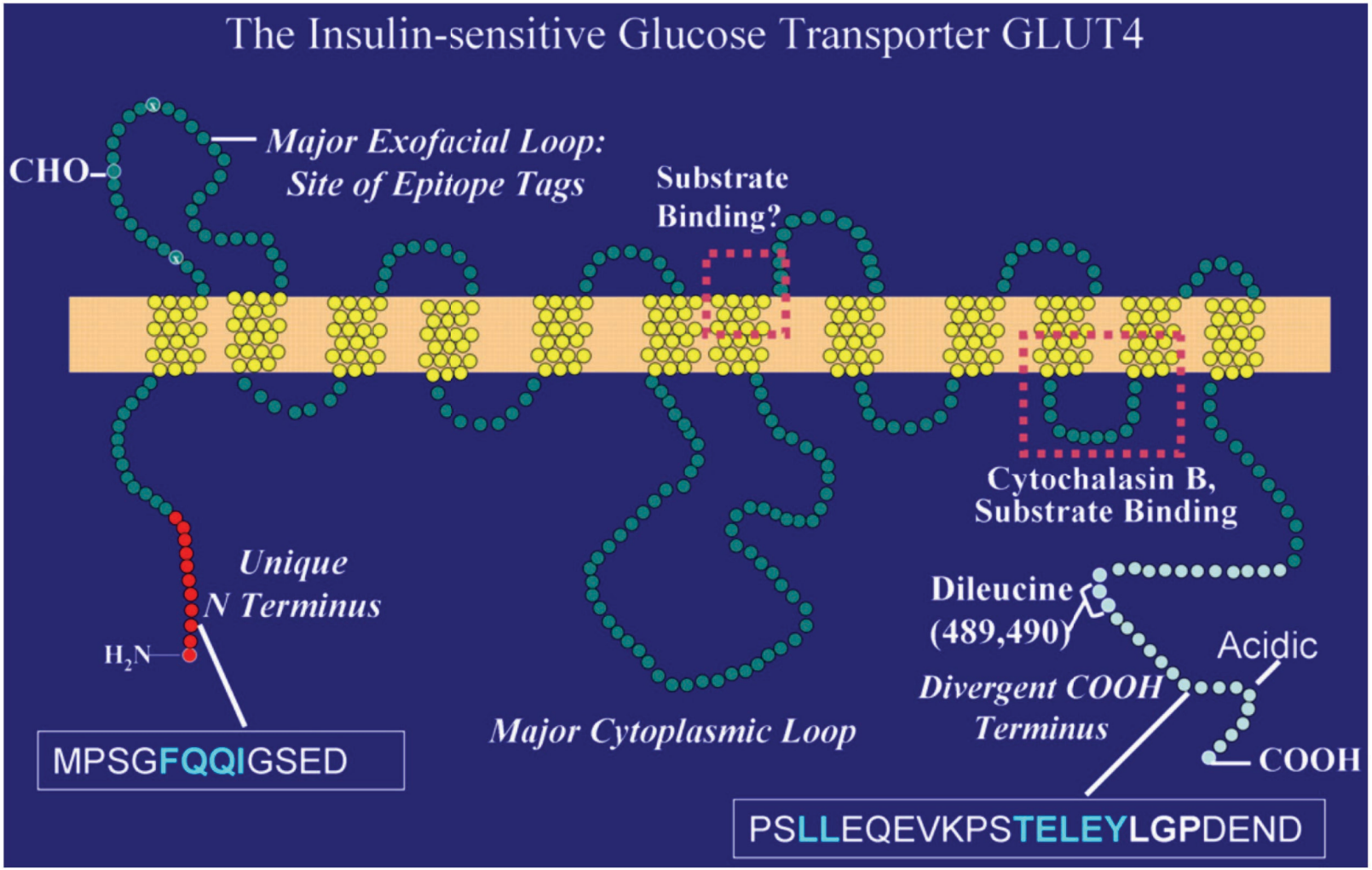

Cell Metabolism 5, April 2007

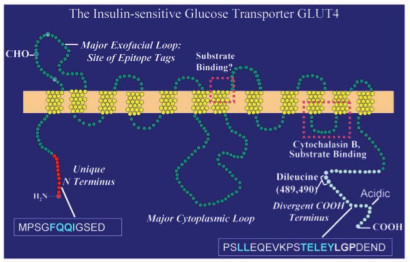

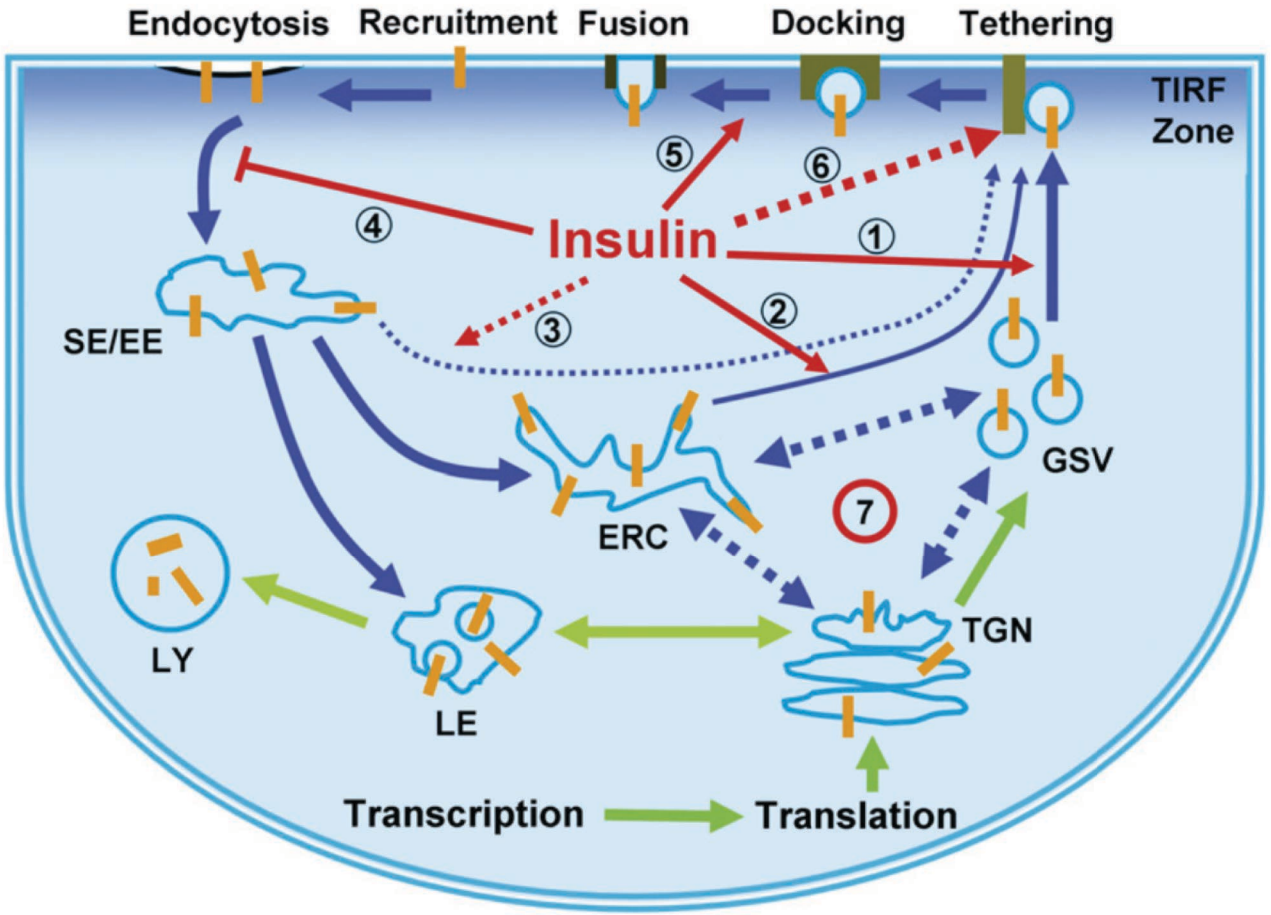

Cell Metabolism 5, April 2007

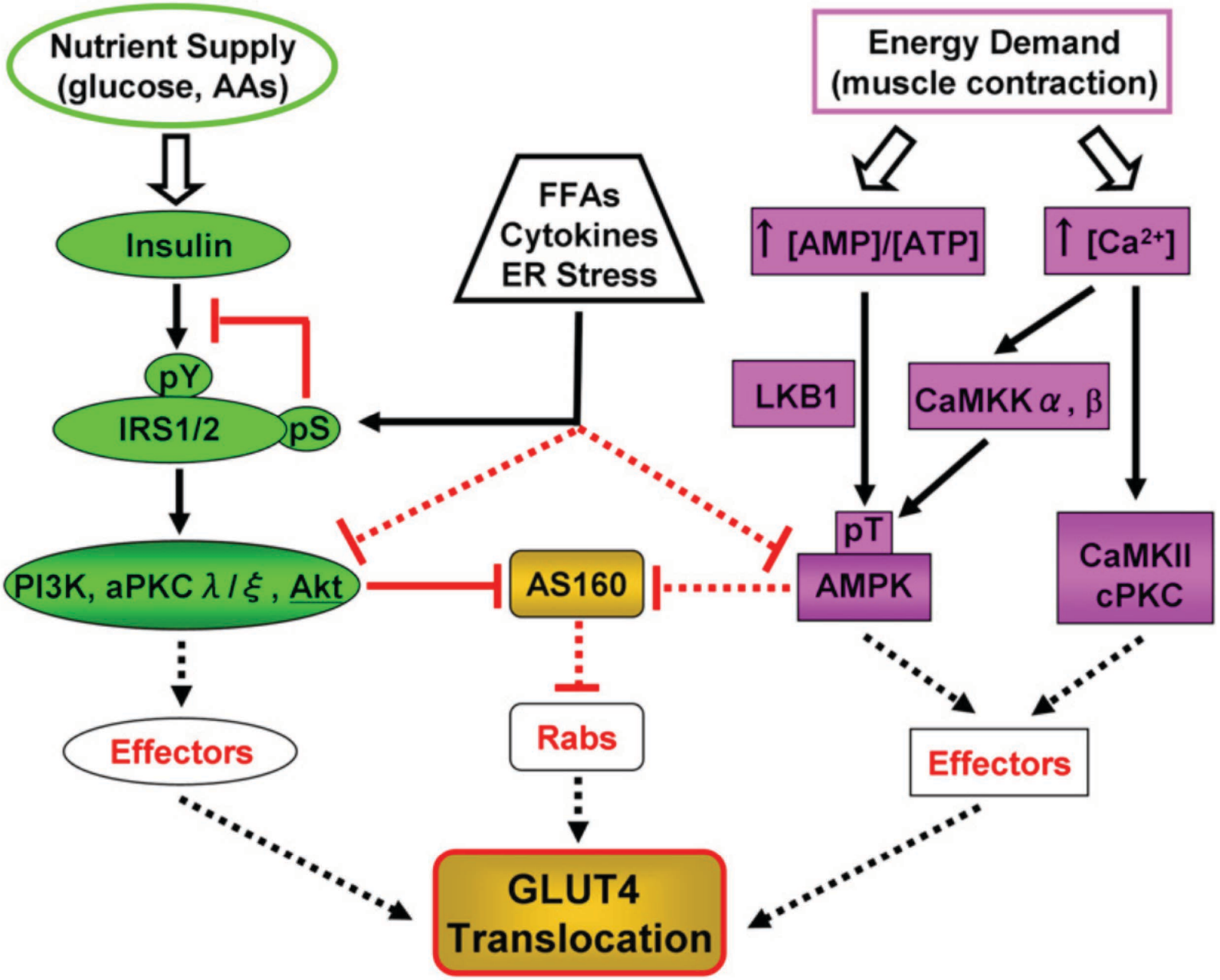

Cell Metabolism 5, April 2007

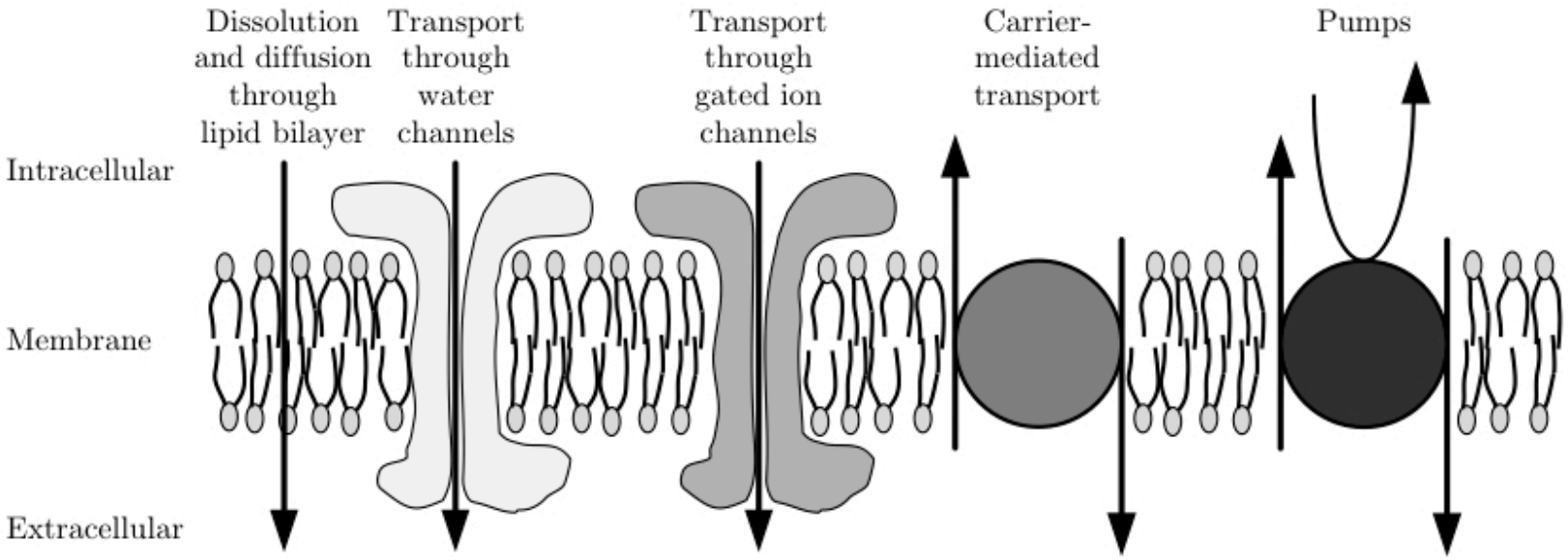
Dissolution and diffusion through lipid bilayer
Transport through water channels
Transport through gated ion channels
Carrier-mediated transport
Pumps
Intracellular
Membrane
Extracellular

Figure 2.19

Glucose transport → Are all the bases covered?

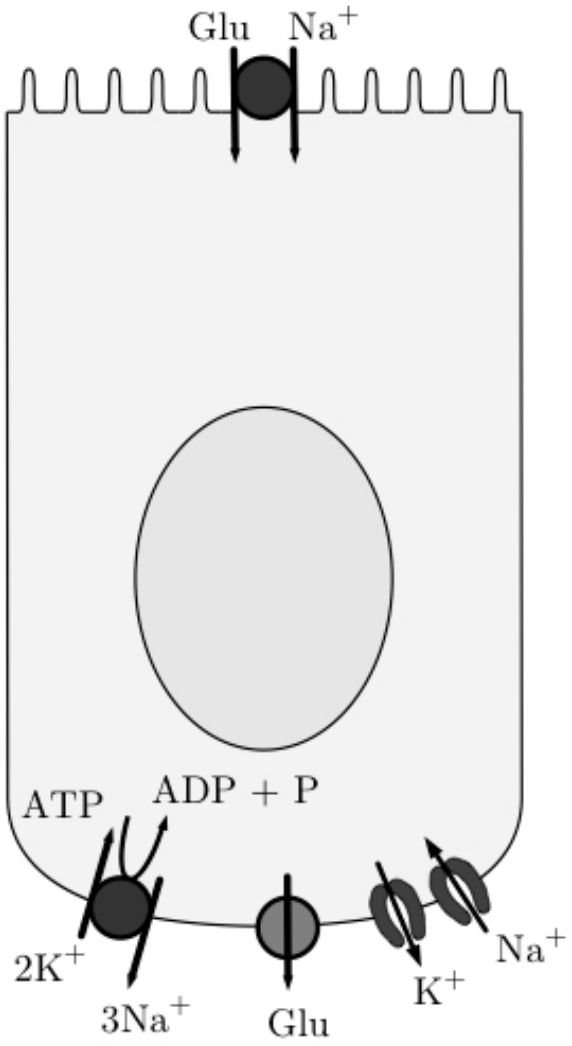

Figure 2.15

→ Need to consider additional aspects (e.g., electrical charge)

Problem

Problem 1. Solute S is transported through a membrane by the simple, symmetric, four-state carrier model. The enzyme can be found in four different states: unbound to solute at either the inside or outside faces of the membrane or bound to solute at either face. The steady-state densities of enzymes in these four states are $\mathfrak{N}_E^i$, $\mathfrak{N}_E^o$, $\mathfrak{N}_{ES}^i$, and $\mathfrak{N}_{ES}^o$ mol/cm^2; the total enzyme density is $\mathfrak{N}_{ET} = \mathfrak{N}_E^i + \mathfrak{N}_E^o + \mathfrak{N}_{ES}^i + \mathfrak{N}_{ES}^o$. The state of the enzyme system is depicted schematically for four different conditions in the following figure.

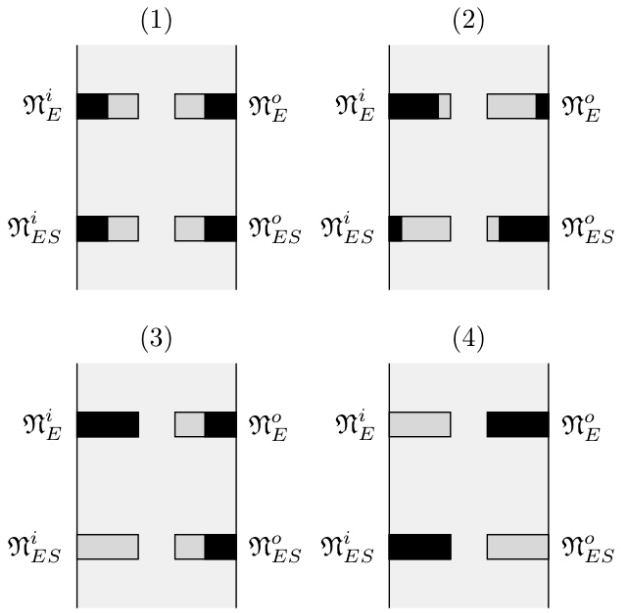

The length of the darker part of the box representing each state is proportional to the fraction of enzyme in that state.

Answer question a-h and give brief explanations for your choice.

a) **True or False:** For all four conditions (1)-(4), $\phi_E = -\phi_{ES}$.

b) **Multiple choice:** Which of the following statements applies to (1):

i) $c_S^i > K$.
ii) $c_S^i = K$.
iii) $c_S^i < K$.

c) **True or False:** The transition from (1) to (3) can be achieved by changing c_S^i only.

d) **True or False:** In (2), $\phi_S > 0$.

Problem

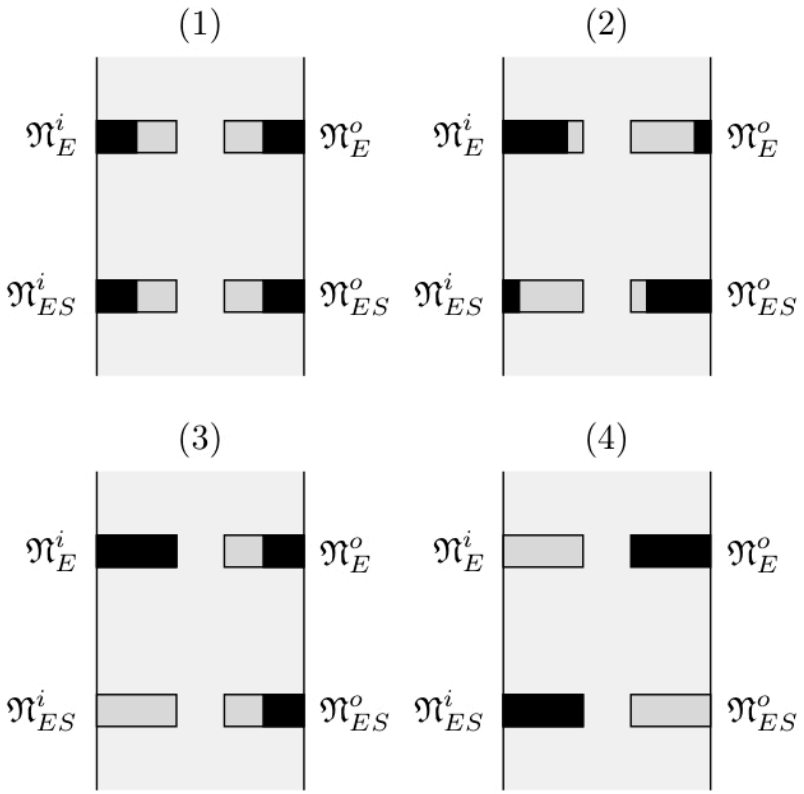

Simple Symetric 4-State Carrier Model

$$\mathfrak{N}_{ES}^i = \left(\frac{\beta}{\alpha+\beta} \right) \left(\frac{c_S^i}{c_S^i + K} \right) \mathfrak{N}_{ET}$$

$$\mathfrak{N}_E^i = \left(\frac{\beta}{\alpha+\beta} \right) \left(\frac{K}{c_S^i + K} \right) \mathfrak{N}_{ET}$$

$$\mathfrak{N}_{ES}^o = \left(\frac{\alpha}{\alpha+\beta} \right) \left(\frac{c_S^o}{c_S^o + K} \right) \mathfrak{N}_{ET}$$

$$\mathfrak{N}_E^o = \left(\frac{\alpha}{\alpha+\beta} \right) \left(\frac{K}{c_S^o + K} \right) \mathfrak{N}_{ET}$$

$$\phi_S = \left(\frac{\alpha\beta}{\alpha+\beta} \right) \mathfrak{N}_{ET} \left(\frac{c_S^i}{c_S^i + K} - \frac{c_S^o}{c_S^o + K} \right)$$

Problem

a) **True or False:** For all four conditions (1)-(4), $\phi_E = -\phi_{ES}$. → True

b) **Multiple choice:** Which of the following statements applies to (1):

i) $c_S^i > K$.

ii) $c_S^i = K$. → ii

iii) $c_S^i < K$.

c) **True or False:** The transition from (1) to (3) can be achieved by changing c_S^i only. → True

d) **True or False:** In (2), $\phi_S > 0$. → False

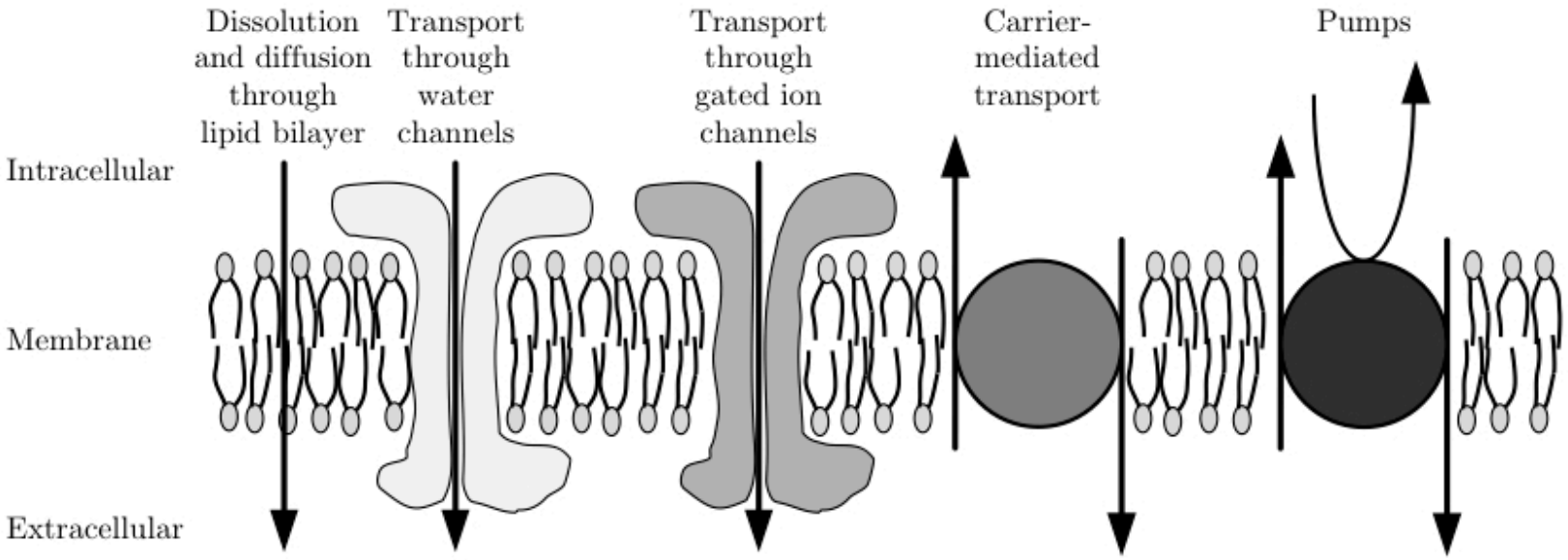
Dissolution and diffusion through lipid bilayer
Transport through water channels
Transport through gated ion channels
Carrier-mediated transport
Pumps
Intracellular
Membrane
Extracellular

Figure 2.19